5.6 EVENT 6: ORBIT 1666 (LARGEST CHARGING POTENTIAL)

Overview Data, 93.02.09, Prince Albert

The overview data for the particle measurements from orbit 1666 are presented in Figure 5.6.1. This event represent one of the largest observed charging levels observed in the Freja data set. The ions are lifted in energy between 0916:00 - 0919:00 UT (panels 1-3). The event is associated with enhanced fluxes of high energy electrons which are part of an auroral inverted-V event (panel 7). The whole event occurs during eclipse (panel 4). The MATE measures only the integrated flux during this orbit.

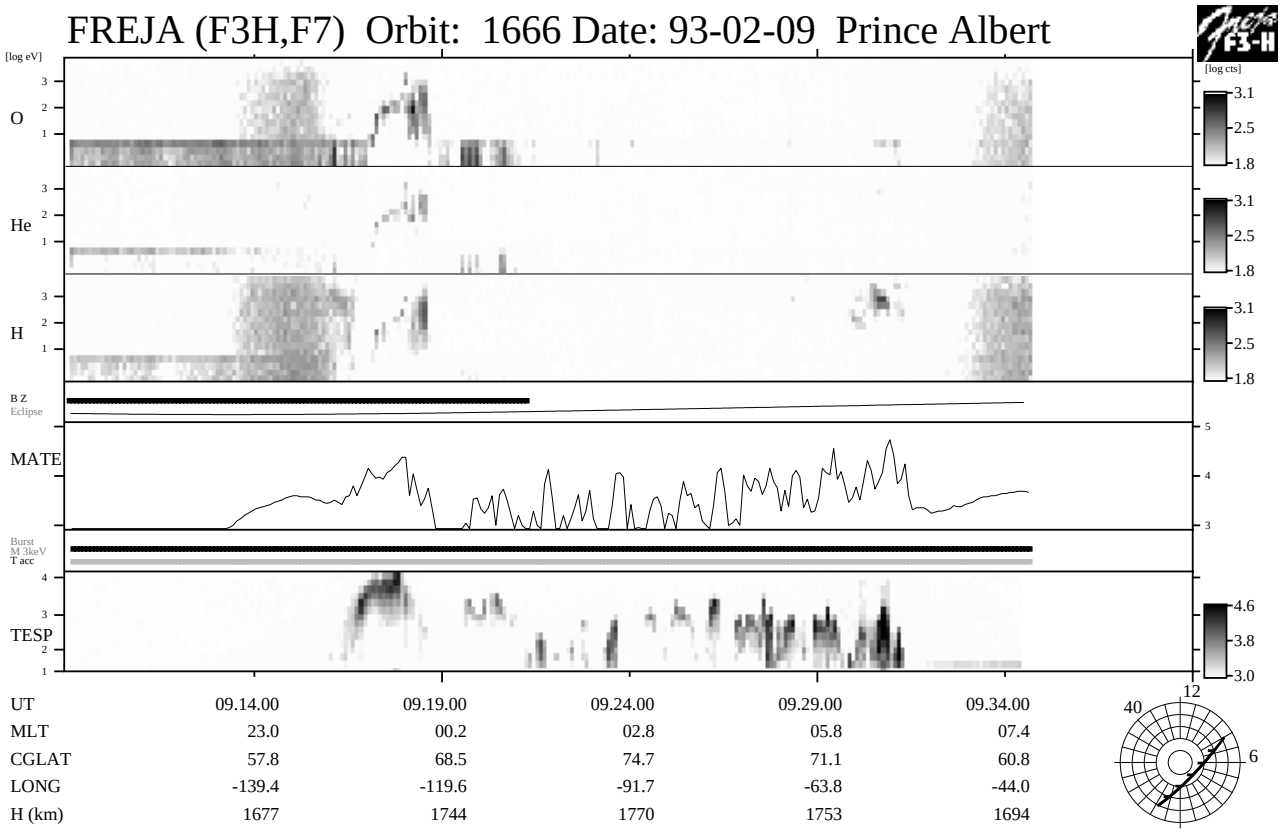

Figure 5.6.1: Overview particle data from the orbit 1666. This orbit reveals one of the highest negative charging levels detected in the Freja data set near 0918:00 UT during eclipse conditions. A clear intense auroral inverted-V event is associated with the charging event.

Figures 5.6.2 and 5.6.3 display the blow up of the particle and plasma wave data around the uplifted ion event. Densities during the charging event vary between $1\text{-}2\cdot10^{8}$ m^{-3} according to the upper cutoff of the HF emissions (panel 1, Figure 5.6.3). In this case the thermal plasma density indeed do decrease when the charging event appears. The ion energy attains values to about -2000 V near 0918:00 UT (panel 1, Figure 5.6.2), a time when the energetic electron fluxes becomes as most intense and the peak energy rise to its largest value (panels 5 and 7, Figure 5.6.2).

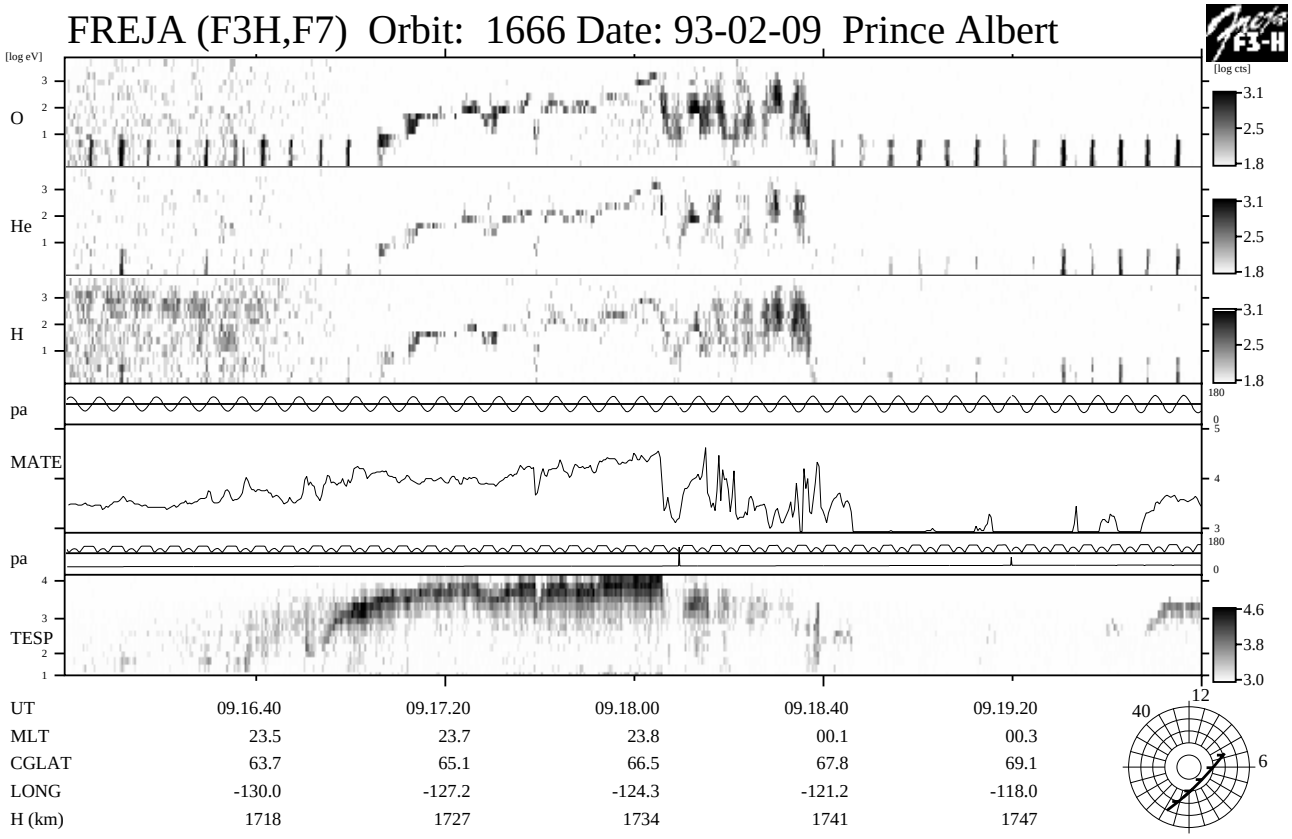

Figure 5.6.2: A blow up of the data around the high level charging event on orbit 1666. The O^+ data (panel 1) show contamination of presumably MeV electrons when maximum charging takes place near 0918:00 UT. Very intense inverted-V electron fluxes (panel 7) matches the time of maximum charging as well.

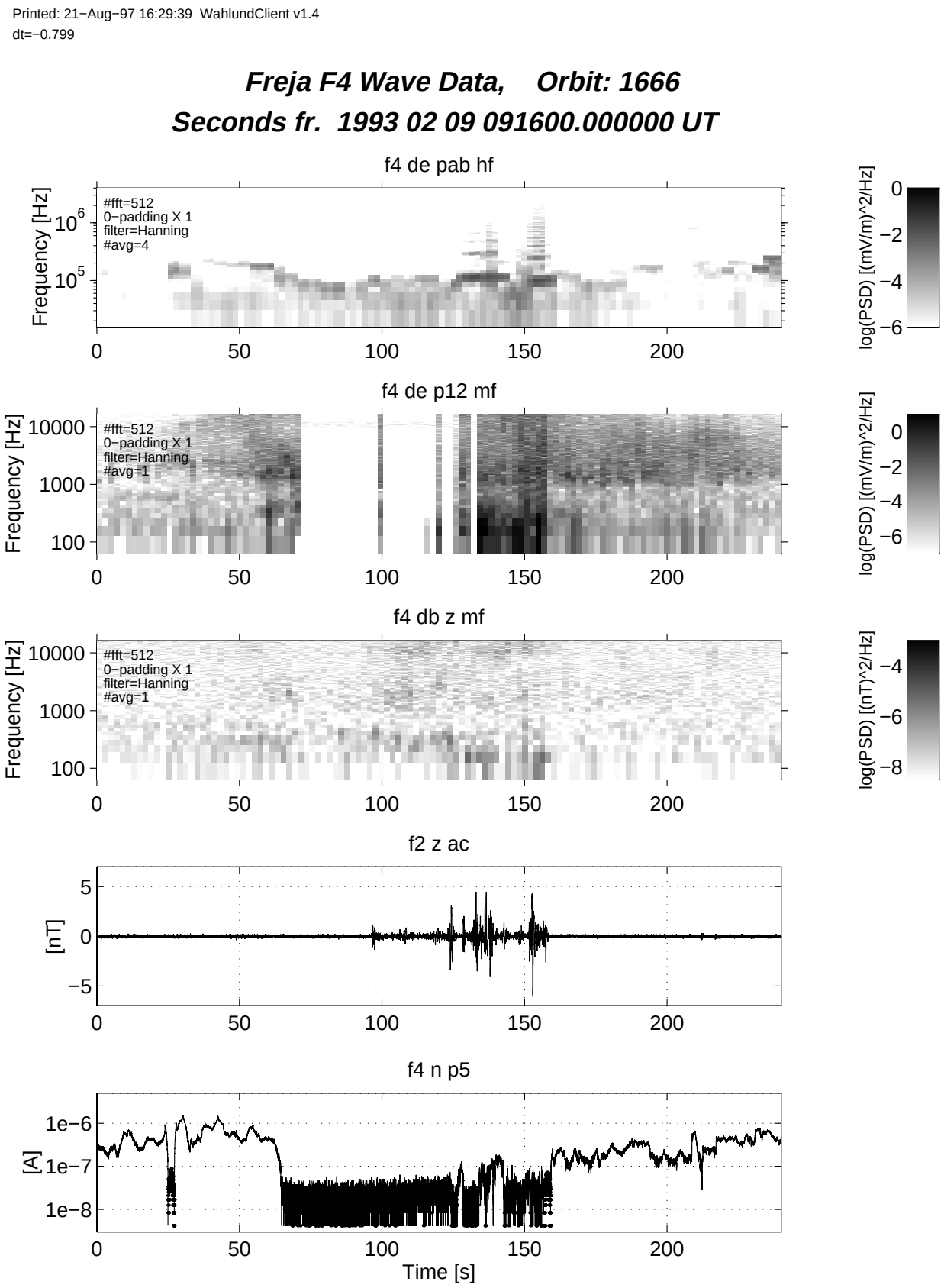

Figure 5.6.3: The plasma density falls to low values during this charging event as indicated by the upper cutoff of the electrostatic whistler type waves around +100 s in panel 1. The MF electric plasma wave data becomes very disturbed during the event, and the Langmuir probe drops due to that no thermal electrons can reach the probe (nor Freja).

Detailed Particle Distributions

Detailed TESP spectra during the event are displayed in Figures 5.6.4a and 5.6.4b. The inverted-V peak becomes displaced upward in energy during maximum charging (panels 3 and 4 in Figure 5.6.4a; panels 1 - 3 in Figure 5.6.4b), and the peak energy is probably even above maximum measured energy (25 keV). The peak flux, on the other hand, stays rather constant during the event. The last panel in Figure 5.6.4b, which is after the time of charging, show evidence of field-aligned suprathermal electron bursts in the energy range 30 - 1000 eV.

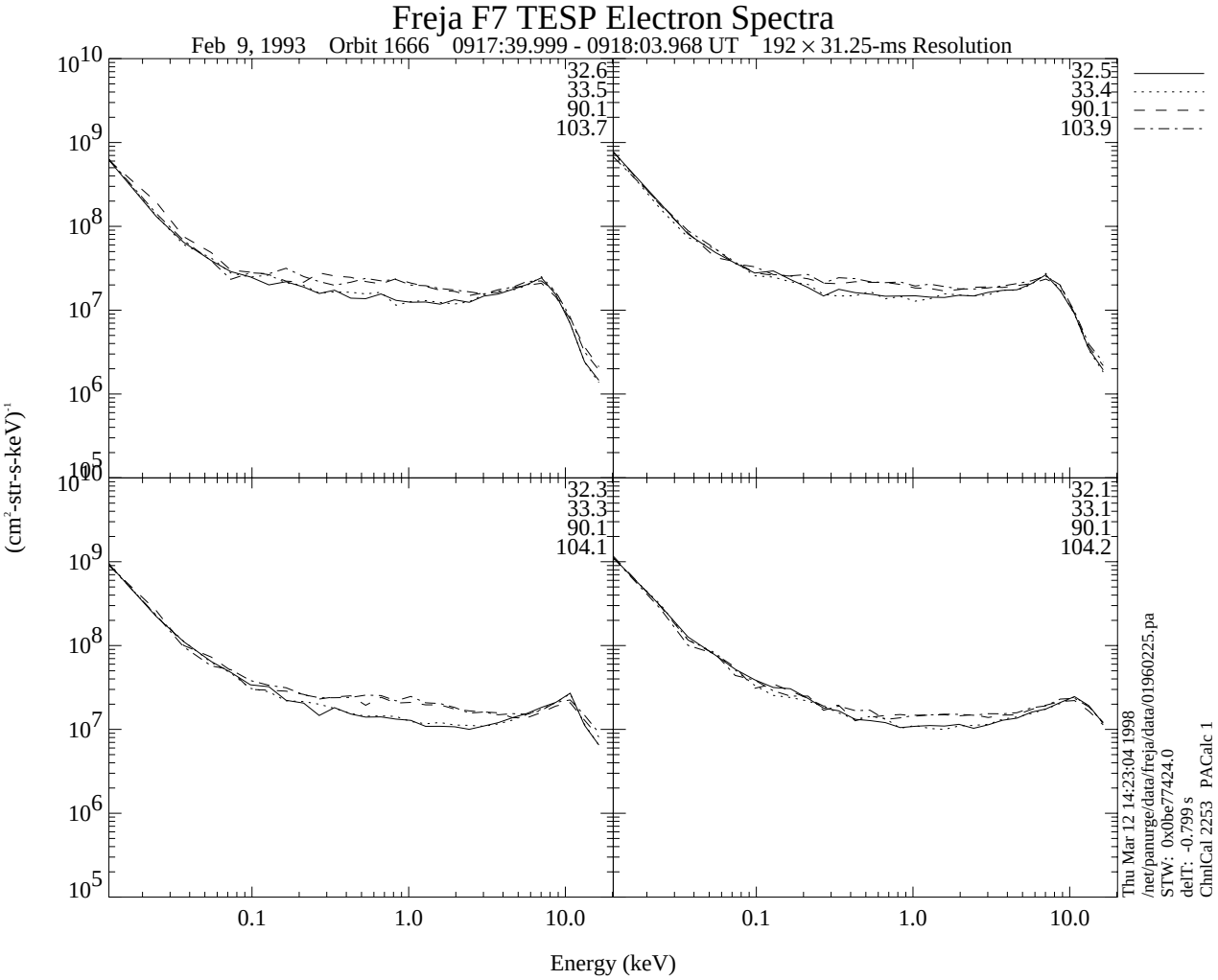

Figure 5.6.4a: TESP electron spectra during the charging event. Maximum charging occurs in panel 3 in the following Figure (Figure 5.6.4b), where the inverted-V peak reaches probably much above maximum measured energy (25 keV).

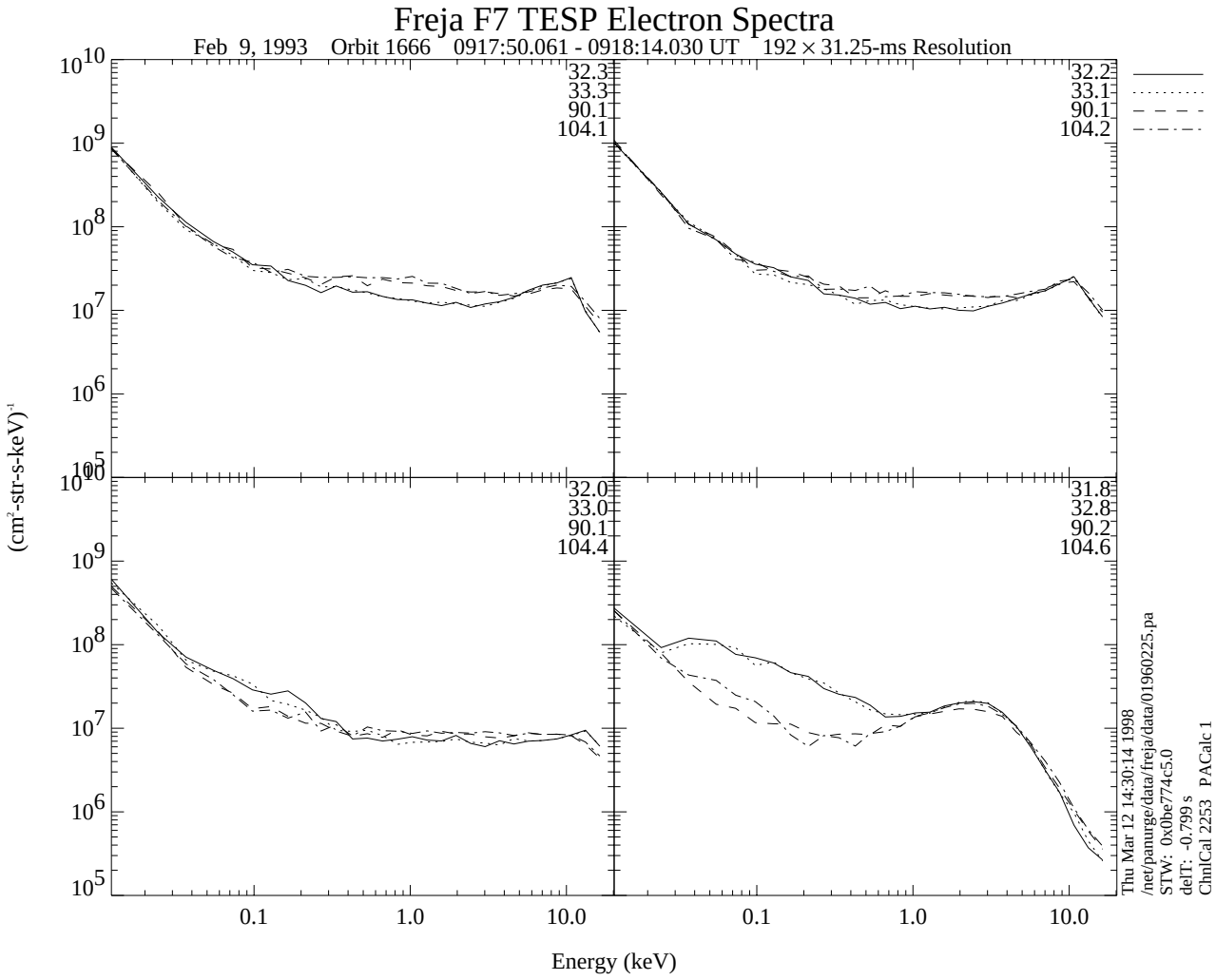

Figure 5.6.4b: See Figure 5.6.4a for text.

The detailed ion distributions around maximum charging are most probably contaminated by large fluxes of high energy electrons in the MeV range. Nevertheless, charging levels up to -1800 V can be inferred from panel 6, where after an ion conic distribution is detected.

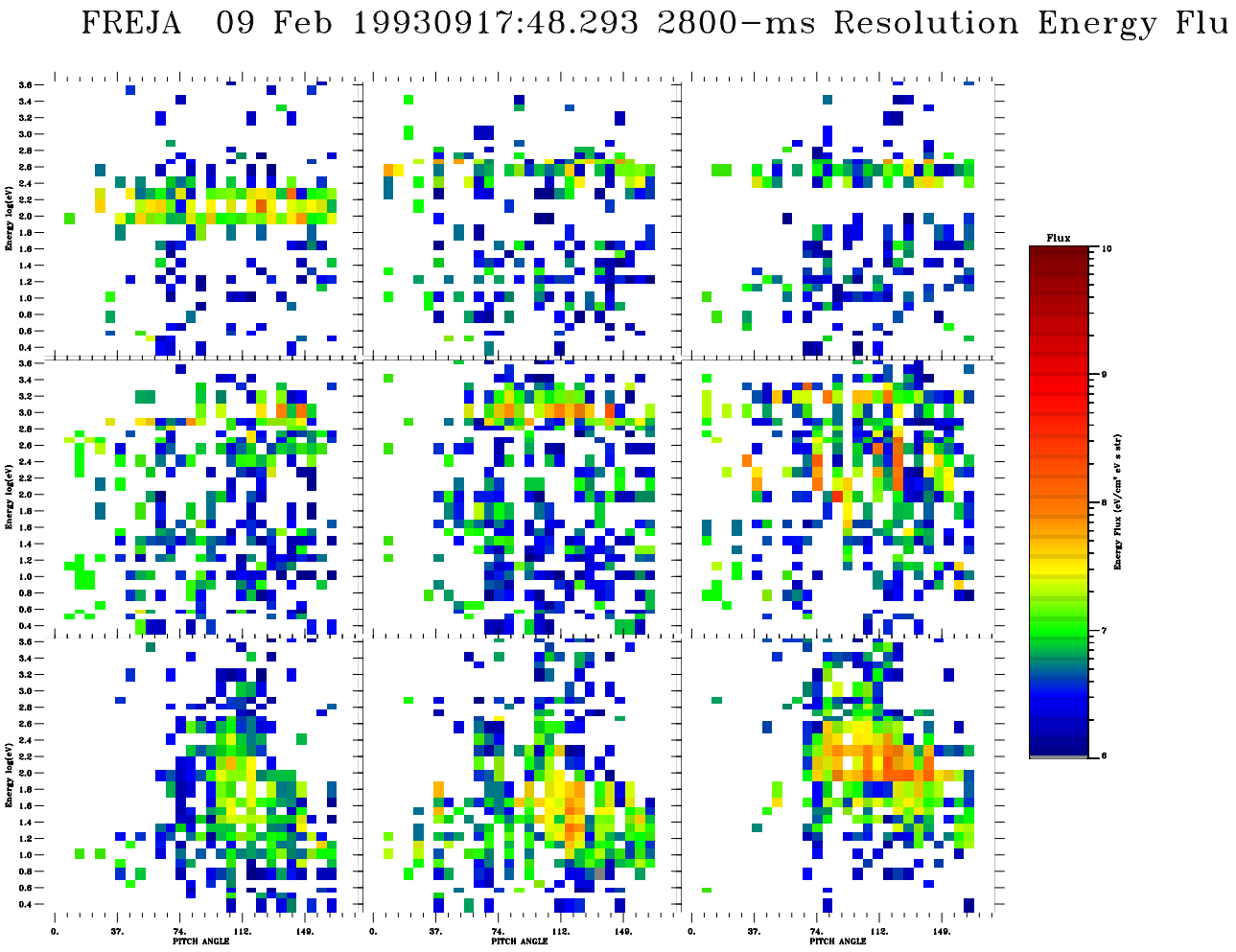

Figure 5.6.5: The O^+ distributions around maximum charging (panel 6). Negative charging levels of -1800 V is inferred.

Conclusions from orbit 1666:

- Freja charging events may reach very large levels despite the efforts of making the Freja spacecraft as electrically clean as possible, in this case near -2000 V.
- The peak energy of the inverted-V event seemed to control the charging level during this event.
- The TICS instrument showed indications of MeV electron fluxes during maximum charging.
- The plasma density decreased to low values during this charging event.
- There are instrument disturbances due to the charging events in the Langmuir probe, MF and LF electric, and the TICS measurements.

5.7 EVENT 7: ORBIT 1785 (CHARGING DURING SUNLIGHT)

Overview Data, 93.02.18, Prince Albert

The overview data for the particle measurements from orbit 1785 are presented in Figure 5.7.1. This charging event is special in that it occurs during sunlight conditions (panel 4, see SPEE-WP130-TN for a detail account on sunlight charging events) around 0932:00 UT. It is clearly associated with high energy (at least up to 25 keV) electrons belonging to an auroral inverted V event (panel 7). Unfortunately no UV photometer data exist for this event, but we are sufficiently confident in the used geometric calculations based on comparisons of such calculations with the photometer data on other orbits.

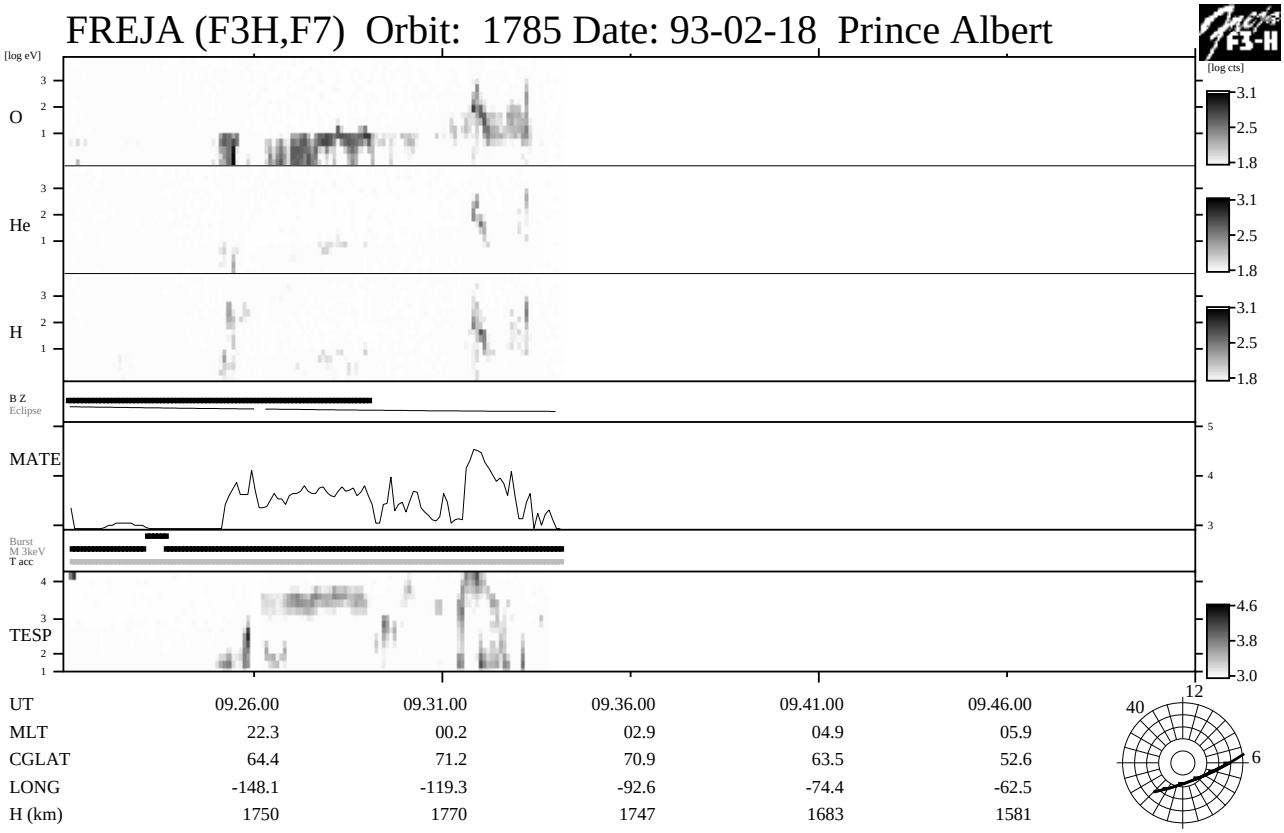

Figure 5.7.1: Overview of the particle data from orbit 1785. A charging event occurs during sunlight conditions around 0932:00 UT, where also a well developed auroral inverted-V structure can be detected (panel 7).

Figures 5.7.2 and 5.7.3 show a blow up of the particle and plasma wave data around the uplifted ion event of interest. The plasma density, as inferred from the HF emissions, stays rather constant during the whole displayed time interval, and estimated densities are nearly constant around $2\text{-}4 \cdot 10^8$ m^{-3}. The LP current clearly drops between +43 s to +73 s, while the HF emissions stays constant. Interestingly, a Langmuir sweep exist at the end of the charging event and one may wonder whether the swept potential +/-12 V caused the spacecraft to discharge. However, the LP current drop also corresponds to a drop in energy and flux of the measured high energy inverted V electrons (panel 7,

Figure 5.7.2). The ion data (panels 1-3, Figure 5.7.2) show a lift in energies of up to -500 V. Between 0931:50 - 0931:55 UT it seems extremely high energy electrons hit "through" to the ion detectors, as is otherwise common during ring current passages. Thus, enhanced fluxes of MeV electrons might be associated with the maximum charging part of this charging event. Charging occurs only when the peak energy of the inverted-V electron population reach above about 5 keV, while no detectable charging exists for lower inverted-V peak energies.

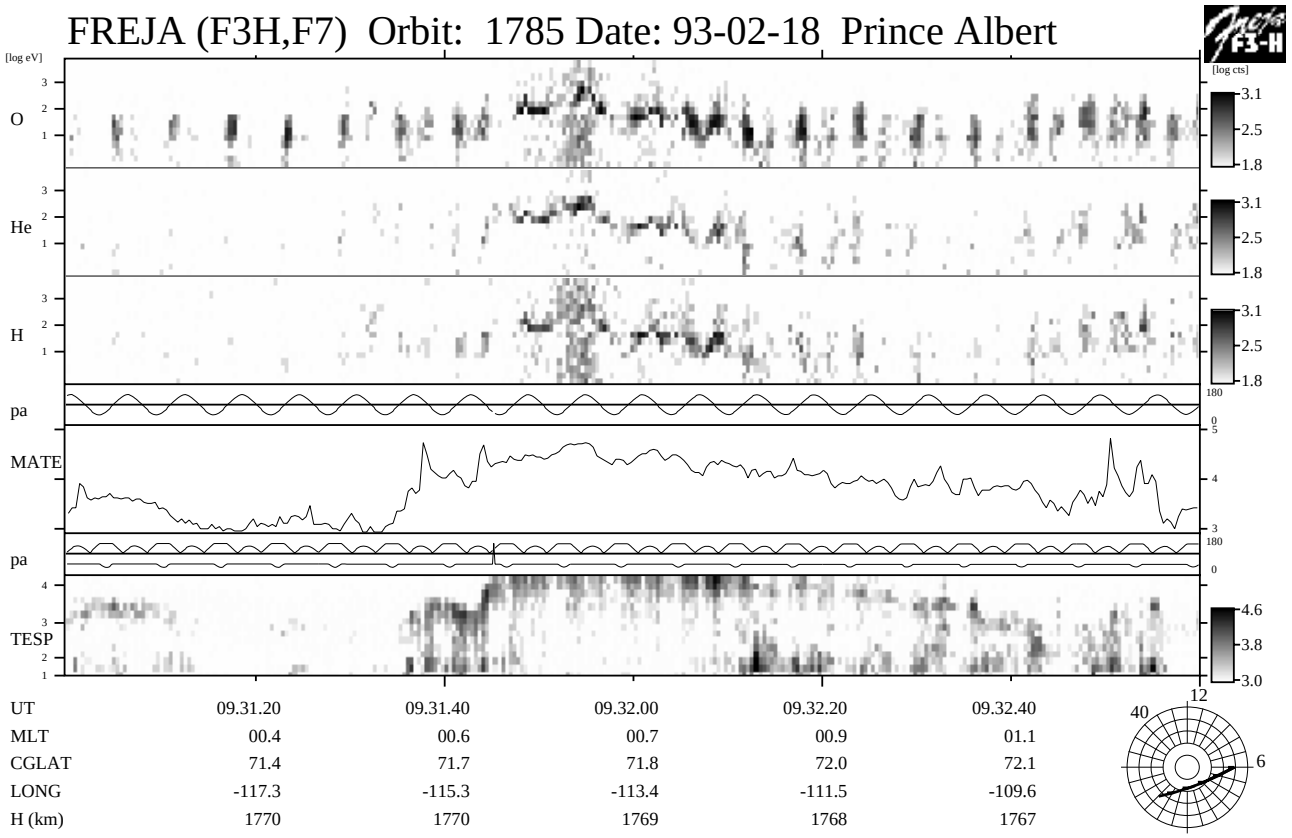

Figure 5.7.2: A blow up of the particle data around the daylight charging event on orbit 1785. It is obvious that the associated auroral inverted-V electron feature (panel 7) reaches at least up to maximum measured energy (25 keV). Contamination most probably from large fluxes of MeV electrons can be detected in all ion channels (panel 1-3).

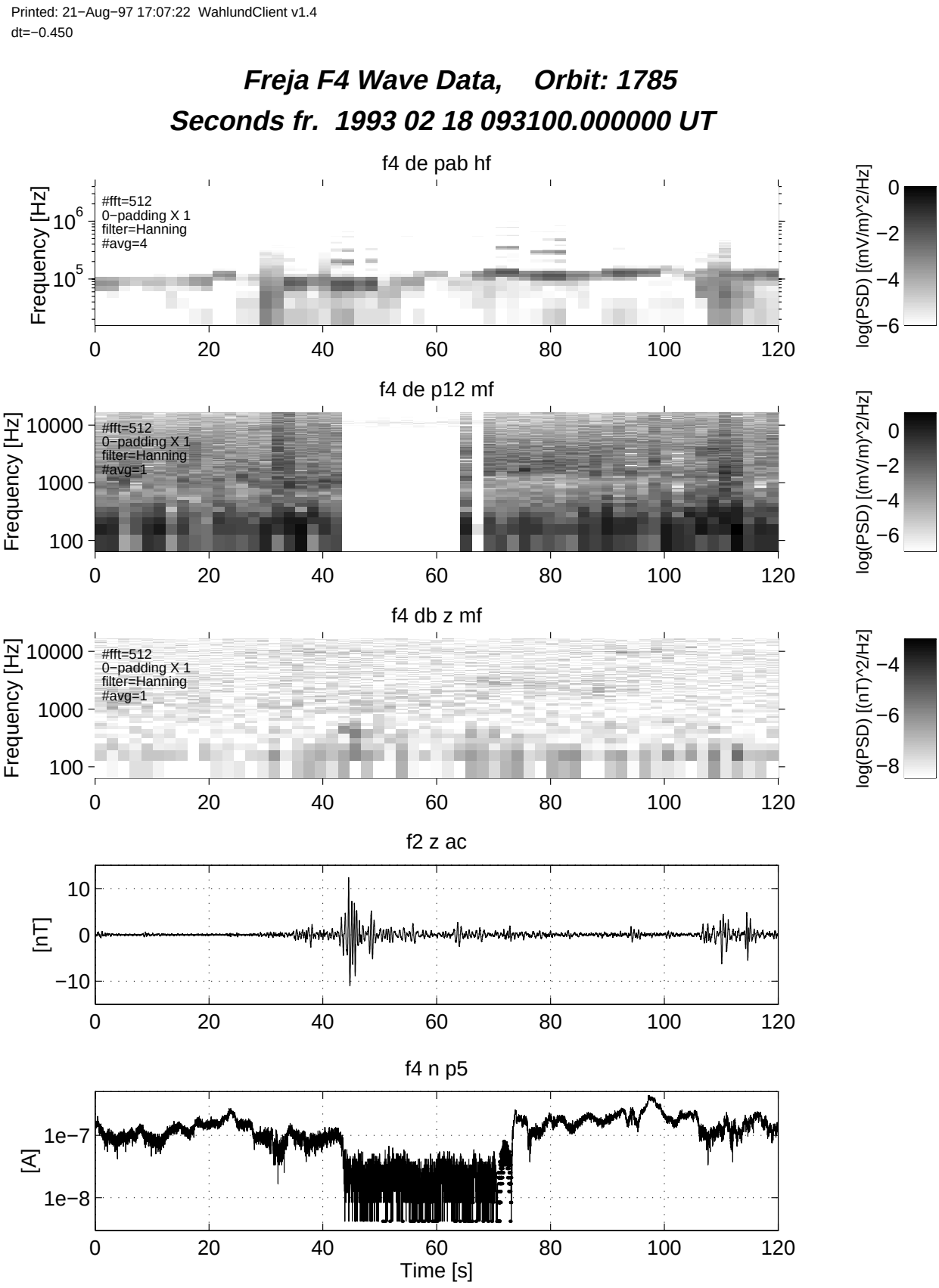

Figure 5.7.3: The cold plasma density is relatively constant during the charging event as inferred from the narrow-band HF Langmuir emissions (panel 1). The charging event is clearly identified by a sharp drop in the Langmuir probe current (panel 5) and disturbances in the MF electric field measurements (panel 2).

Detailed Particle Distributions

Detailed TESP spectra during the charging event are displayed in Figures 5.7.4a and 5.7.4b. Before and after the charging event, field-aligned suprathermal electron beams are detected at energies below 1 keV. These low energy electron beams may inhibit the charging process since maximum yield for secondary electrons occurs around a few hundred eV energy. Unfortunately the inverted-V peak-energy stayed below or around the crossover-yield-threshold energy for Freja charging (few keV) at these occasions, and no final conclusion could be made regarding the inhibiting influence of these low energy electrons. The inverted-V energy peak during the charging event, on the other hand, is probably even above the maximum measured energy of the TESP instrument (25 keV).

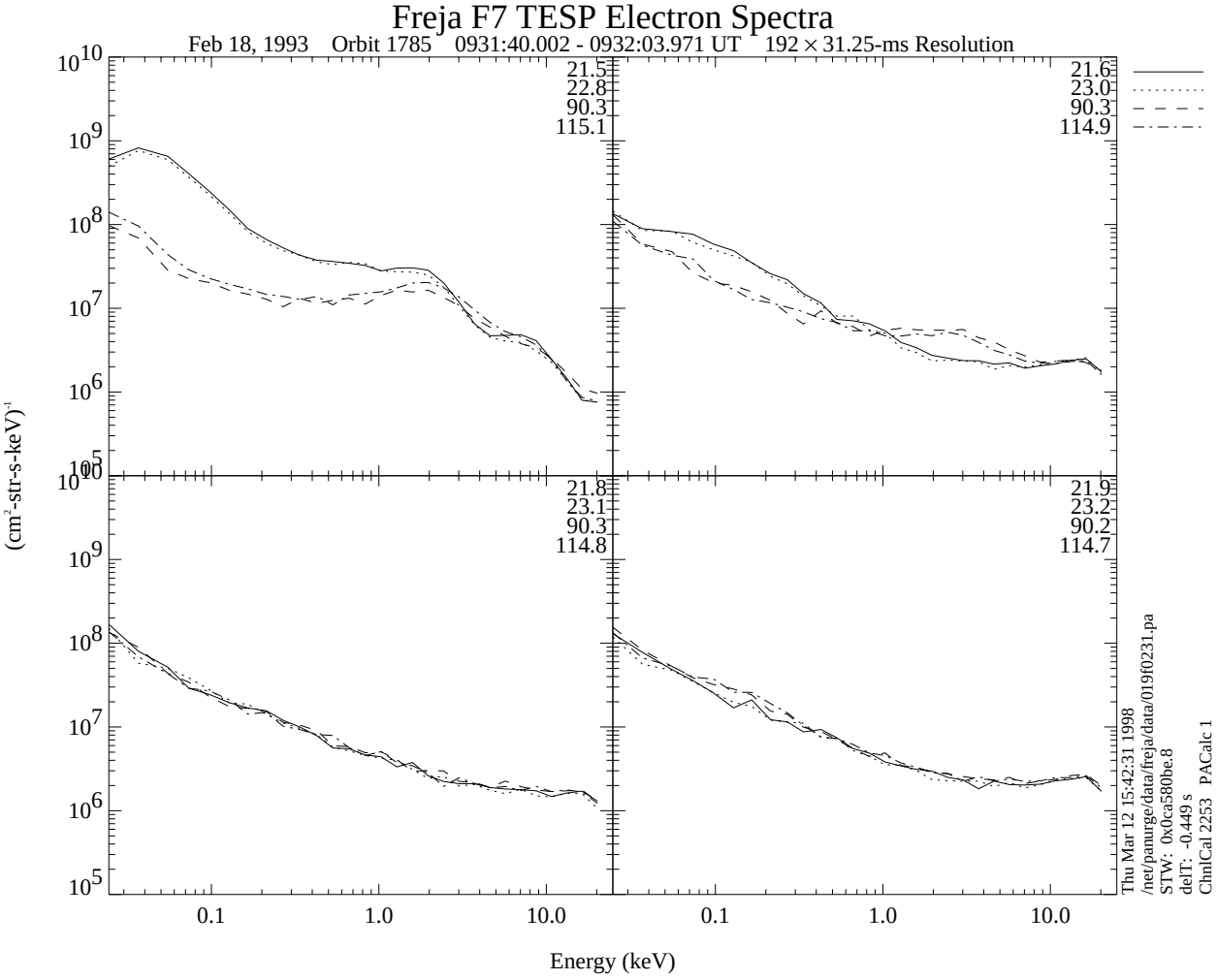

Figure 5.7.4a: TESP electron spectra from the time of the Freja charging event. The inverted-V energy peak reaches up to the maximum measured energy (25 keV) during maximum charging (panel 3).

Detailed ion distributions during the event are shown in Figure 5.7.5a and 5.7.5b. The data is heavily contaminated, most probably by large fluxes of MeV electrons, but charging levels up to -500 V can be inferred.

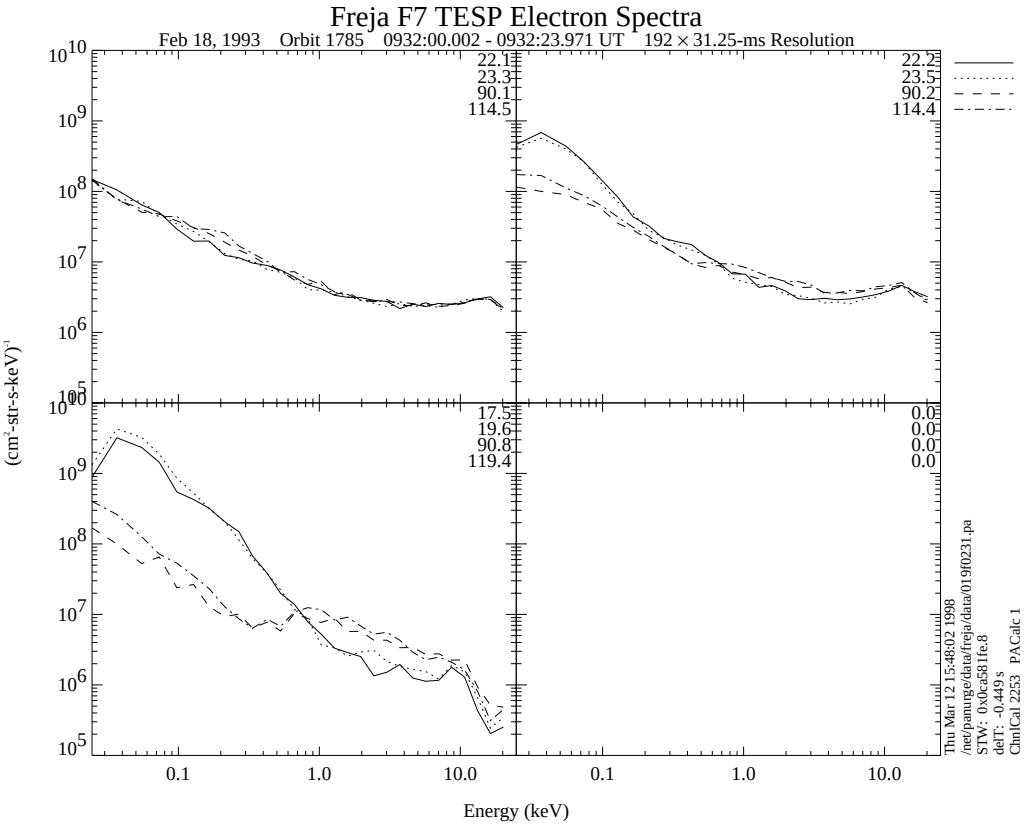

Figure 5.7.4b: TESP electron data. A continuation of Figure 5.7.4a.

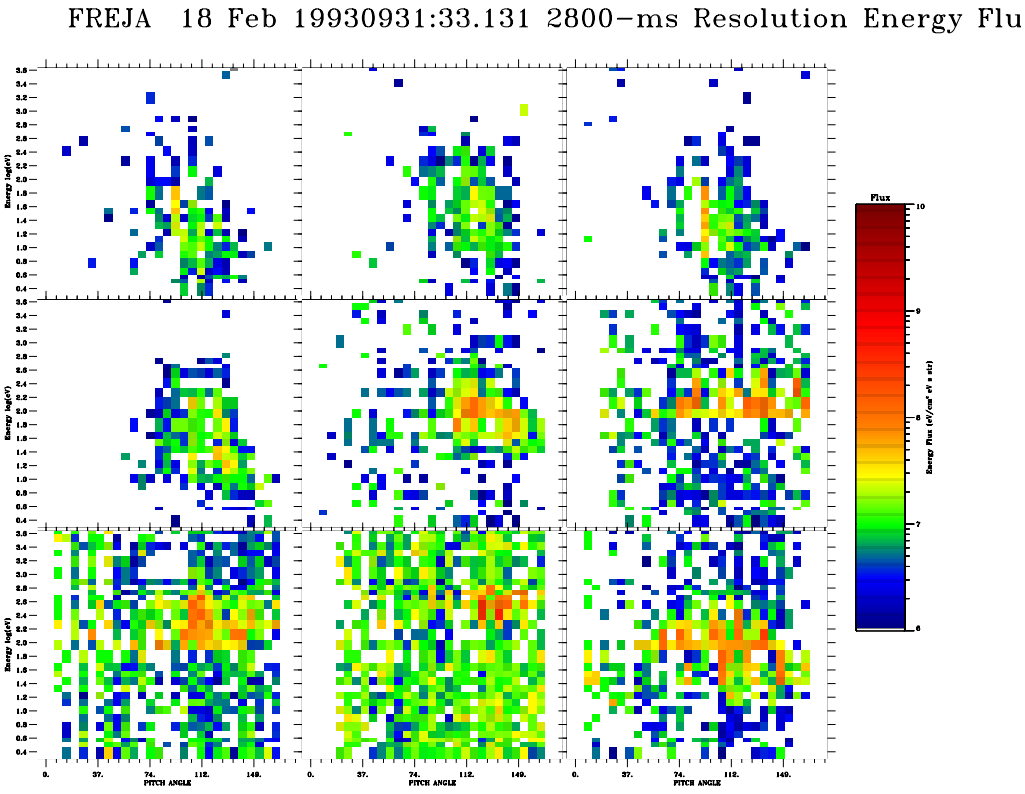

Figure 5.7.5a: Oxygen ion distribution data around maximum charging (panel 8), where negative charging levels of about -500 V can be inferred. The data is heavily contaminated, probably by large fluxes of MeV electrons.

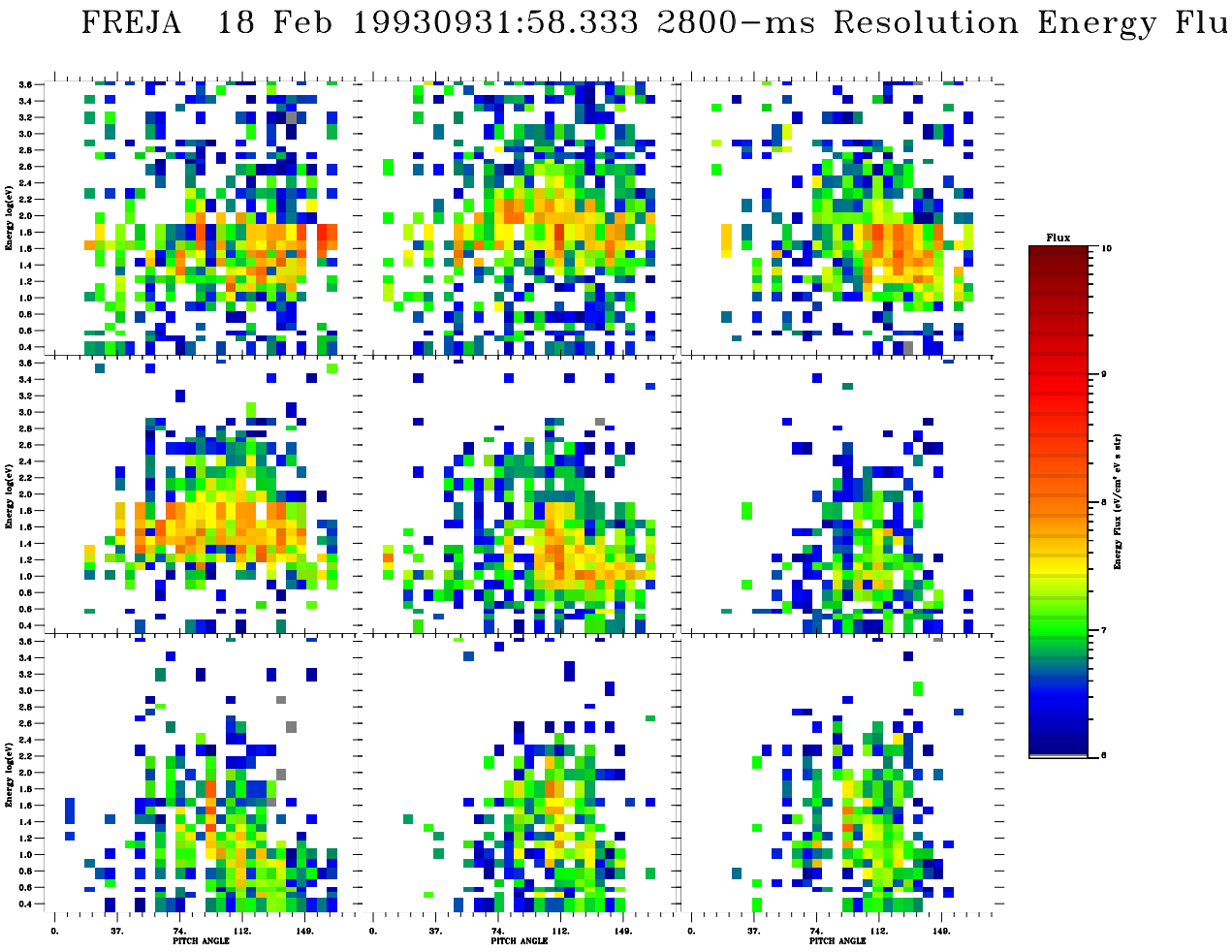

Figure 5.7.5b: Continuation of Figure 5.7.5b.

Conclusions from orbit 1756:

- High level negative charging can occur on Freja when it is situated in sunlight, i.e. despite that large fluxes of photoelectrons are emitted from the spacecraft.
- The inverted-V peak energy is probably above 25 keV and large fluxes of MeV electrons are inferred from the contaminated TICS measurements during maximum charging.
- The plasma density stayed relatively constant during the charging event.
- Charging did not occur if the inverted-V peak energy fell below about a few keV.
- There are instrument disturbances due to the charging events in the Langmuir probe, MF and LF electric, and the TICS measurements.

5.8 EVENT 8: FIVE LOW ALTITUDE SURVEY ORBITS (SUSPECTED CHARGING)

In this section we present the five events of suspected charging of Freja which were found in the low altitude survey orbits (600 - 1000 km). Unfortunately there exist no plasma wave data of reliable quality during these events. These events have been picked out as possible charging events from a database of several hundred low altitude orbits by visual inspection of the survey data. There is no scientific claim made that these low altitude events are real charging events, except for the event on orbit 7945. Neither can we make the claim that charging of Freja is common or not at low altitudes based on this data set. It is merely an indication of that low altitude charging (600 - 1000 km) may indeed have occurred on Freja during auroral conditions. A better study have to wait for the next satellite equipped with suitable instruments, *Astrid 2*, to be launched during December, 1998, into a low altitude polar orbit (about 1000 km).

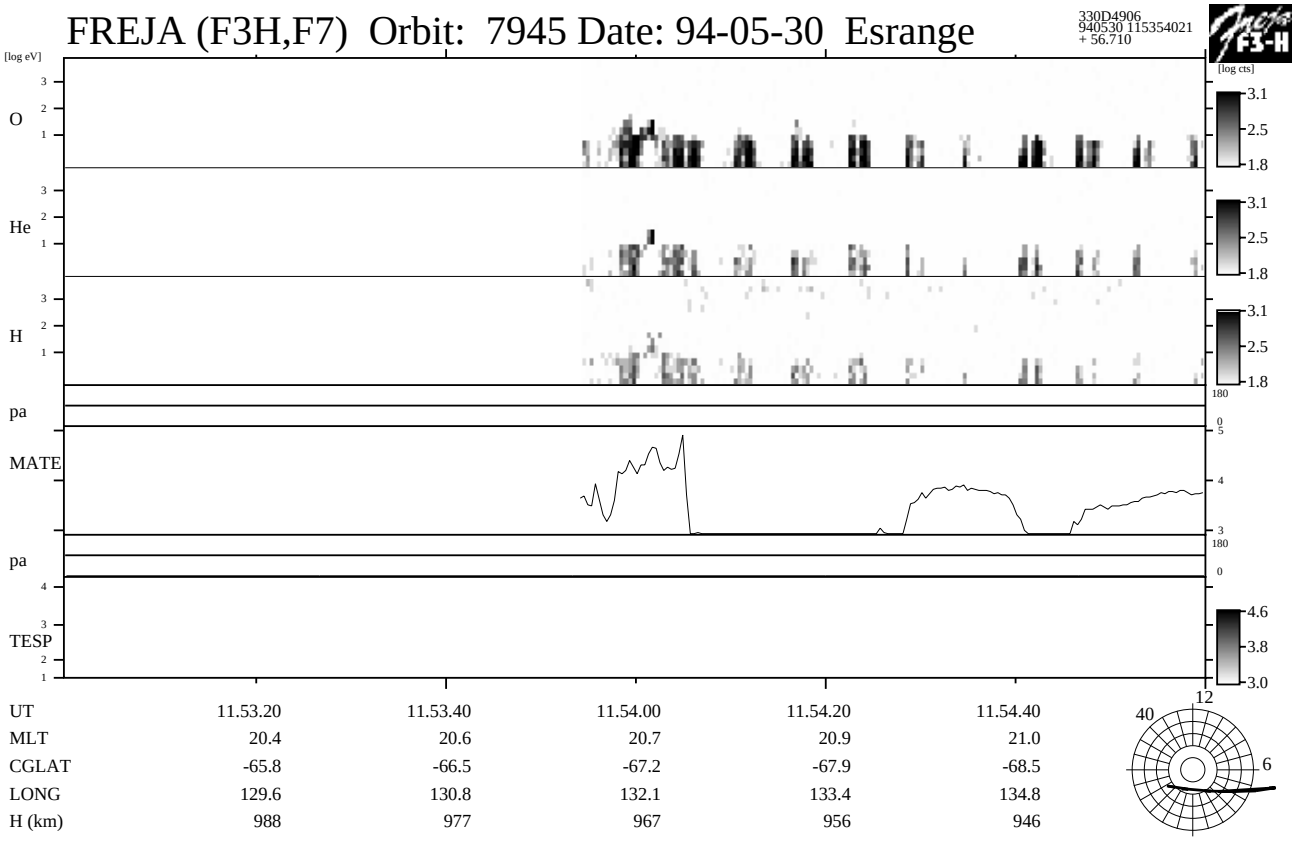

Figure 5.8.1: Orbit 7945. A weak (-10 V) short lived charging event at an altitude of 970 km. The event occurred during eclipse.

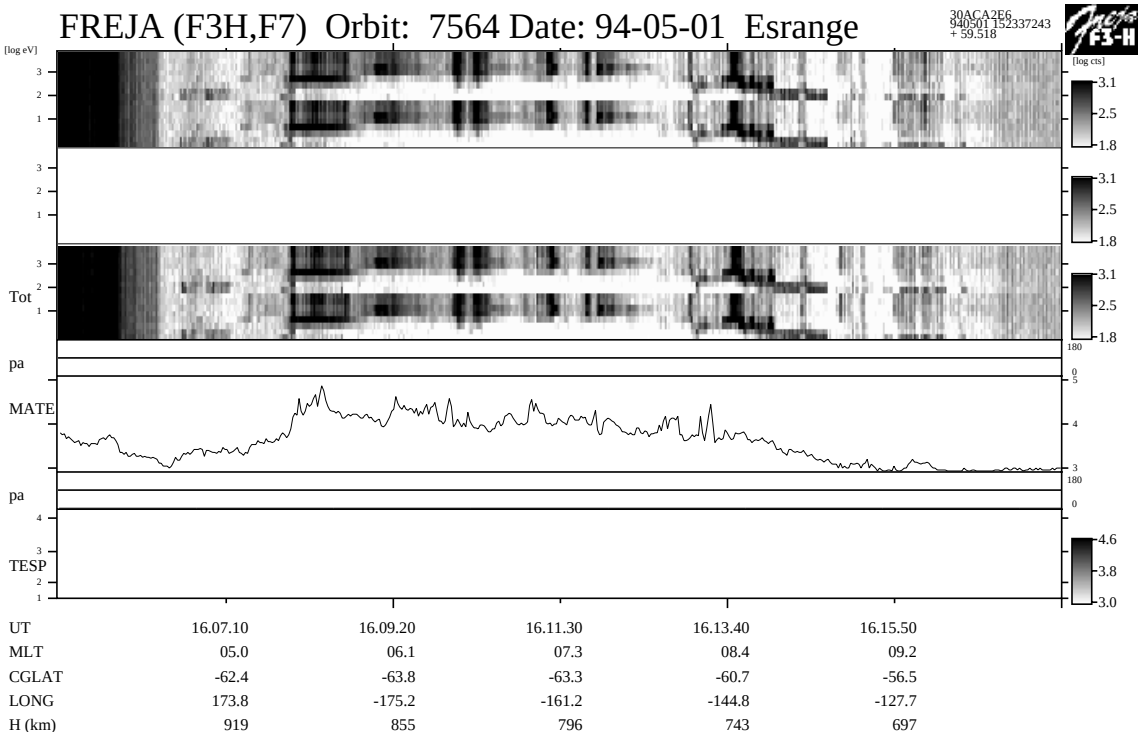

Figure 5.8.2: Orbit 7564. The ion data were unfortunately copied to the high energy part by mistake. The lower portion of the ion data is the correctly measured data, and a possible long duration charging event of about -10 V can be seen. The high energy (MATE) integrated electron flux indicate that high energy electrons could have been present during most of this event. The event occurred mainly in sunlight (from about 1609:00 UT). The altitude varies between 740 km - 900 km.

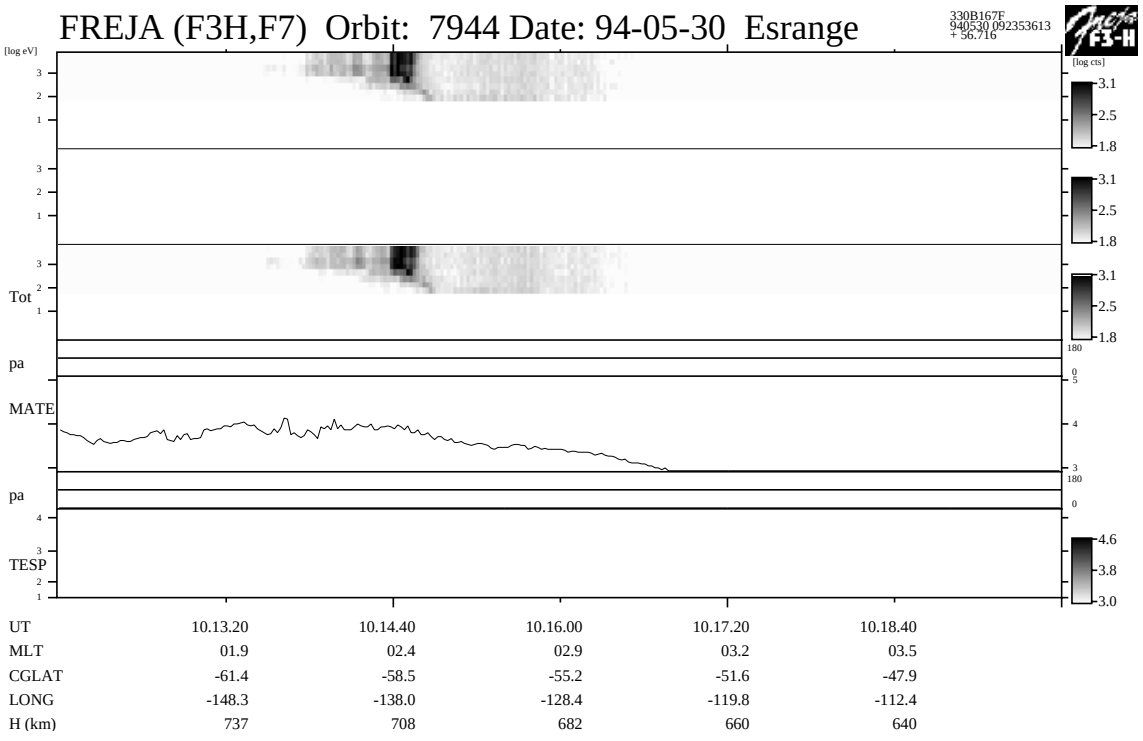

Figure 5.8.3: Orbit 7944. A possible charging event in eclipse near 1014:00 UT (700 km), which is associated with a significant integrated energetic electron flux as measured by the MATE instrument. Charging up to several hundred Volts negative could be inferred if this is a charging event. The event could also be due to ion precipitation.

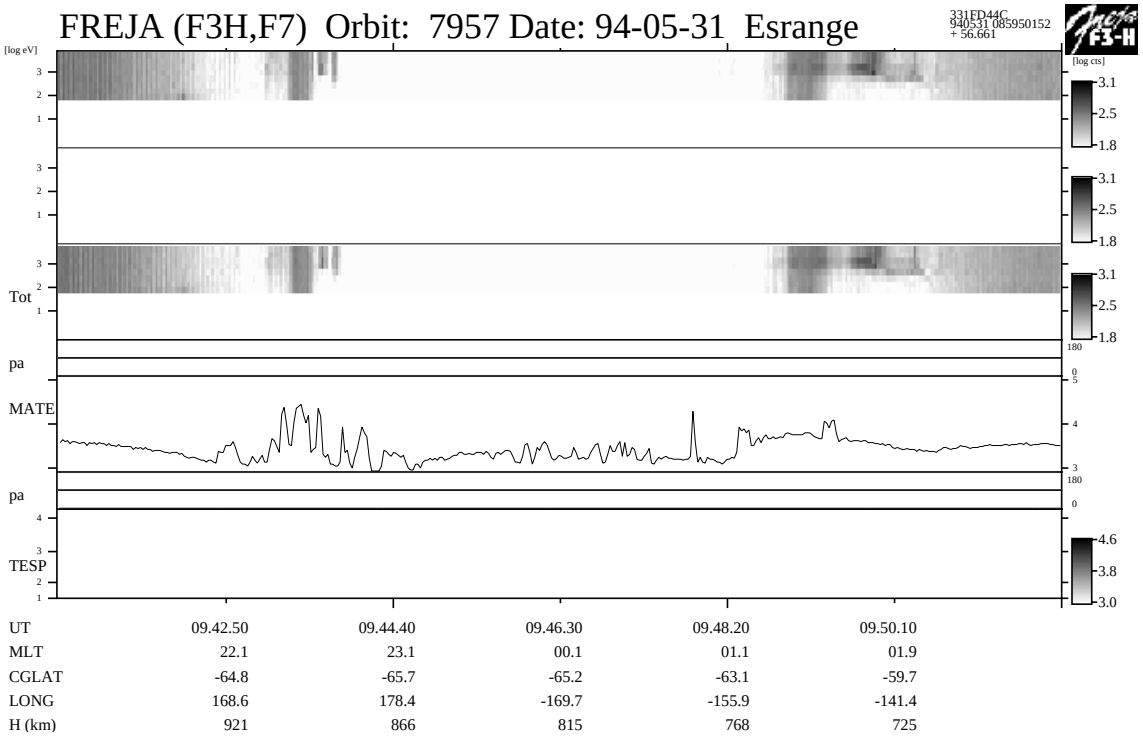

Figure 5.8.4: Orbit 7957. Possible charging event in eclipse near 0943:30 UT and near 0950:00 UT (more probable). Inferred charging levels would in that case be several hundred Volts negative. The first event have an integrated energetic electron flux more characteristic of field-aligned electron bursts (i.e. not charging), while the later event have characteristics of more stable inverted-V type electron precipitation. The events occurred at altitudes around 900 km and 725 km respectively.

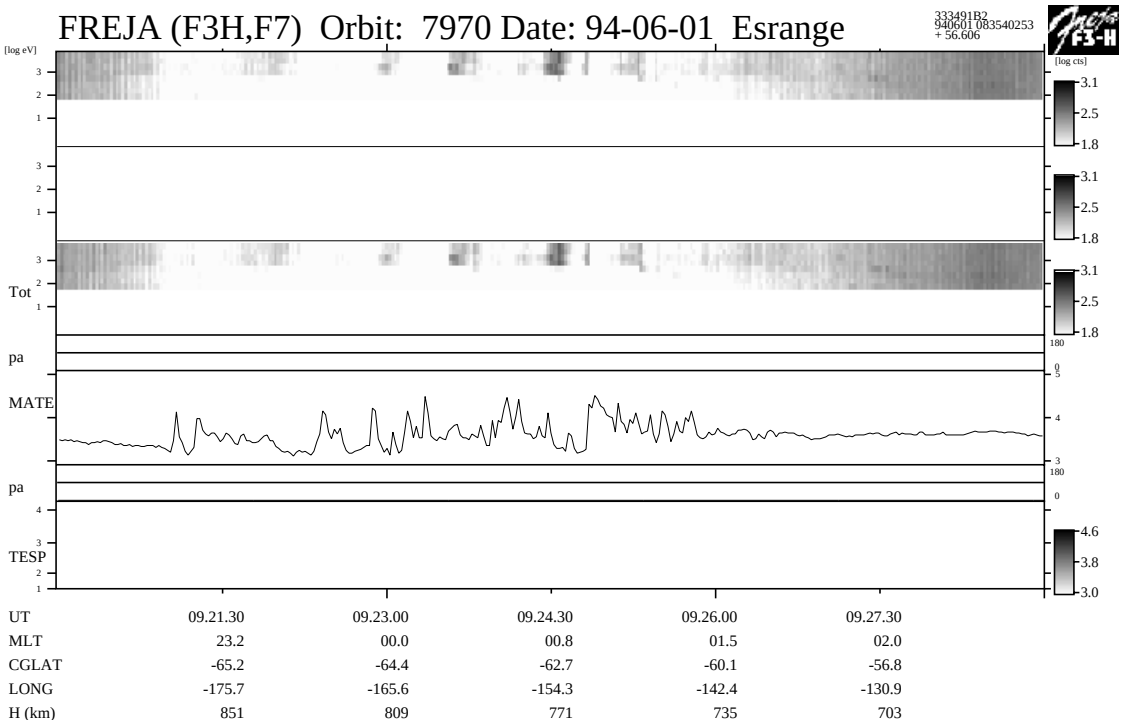

Figure 5.8.5: Orbit 7970. Possible multiple charging events in eclipse of about a few hundred Volts negative. However, the integrated energetic electron flux as measured by the MATE detector (panel 5) show fluctuating characteristics usually more related to low energy field-aligned electron bursts. The altitudes varies between 725 km - 875 km.

5.9 EVENT 9: ORBIT 736 (VARIATION WITH PLASMA DENSITY)

Overview Data, 92.12.01, Esrange

The overview data for the particle measurements from orbit 736 are presented in Figure 5.9.1, and in somewhat more detail in 5.9.2. Three consecutive charging events occur during eclipse in the time period 0034:30 - 0038:00 UT, and all three events are associated with apparently similar energetic electron spectra. Despite this fact, the first charging event near 0035:20 UT reaches a somewhat larger charging level (-50 V) than the two that follows (-5 to -10 V, at 0035:50 UT and 0037:10 UT respectively). The middle event have a somewhat lower electron peak energy, but somewhat larger electron peak flux.

The plasma wave data is presented in Figure 5.9.3. The electron densities during the three events as inferred from the narrow-band HF emissions are $1.0\text{-}1.5 \cdot 10^8$ m^{-3}, $7\text{-}8 \cdot 10^8$ m^{-3} and $5 \cdot 10^8$ m^{-3} respectively. Thus, a factor of 5-8 in density increase is associated with a decrease in the charging level by a factor 5-10. Thus, the electron density might determine the charging level to a greater extent during this event.

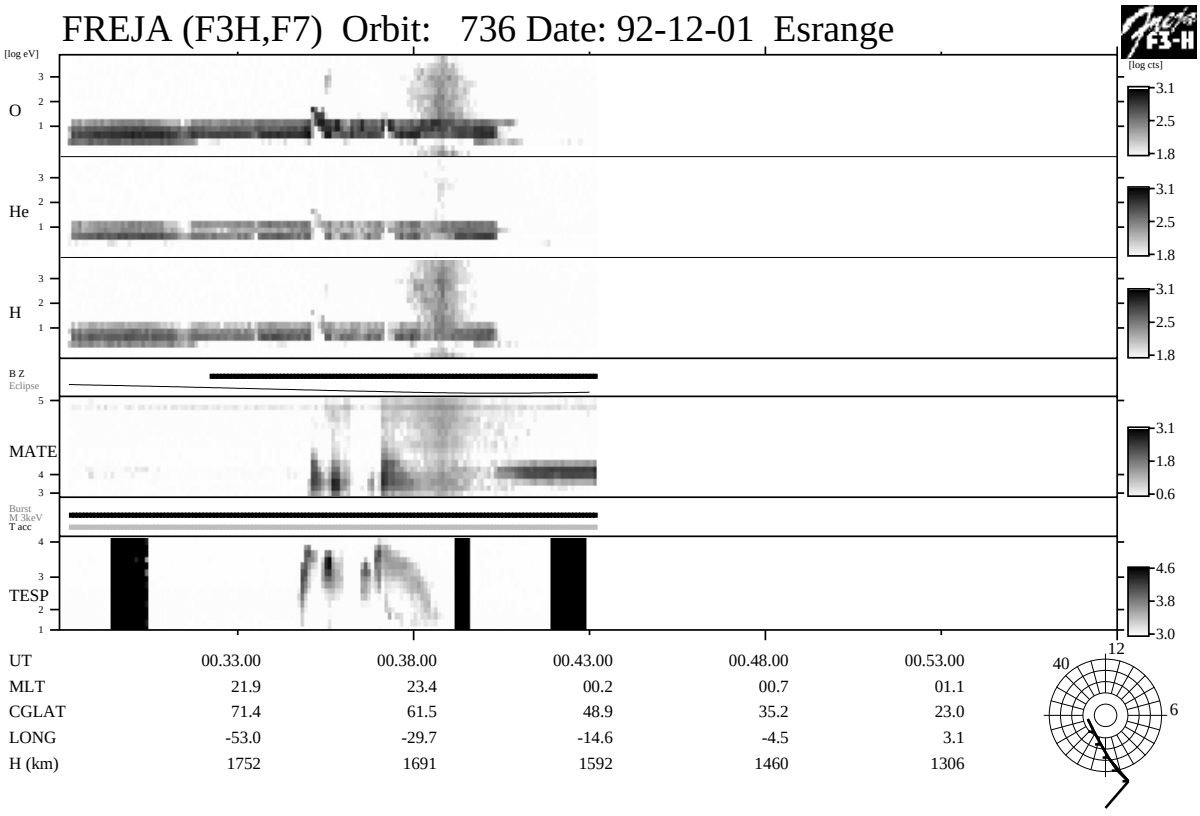

Figure 5.9.1: Overview particle data for orbit 736. Three consecutive relatively low level charging events exist between 0034:00 UT - 0038:00 UT during eclipse conditions. Both MATE (panel 5) and TESP (panel 7) electron data existed during this orbit.

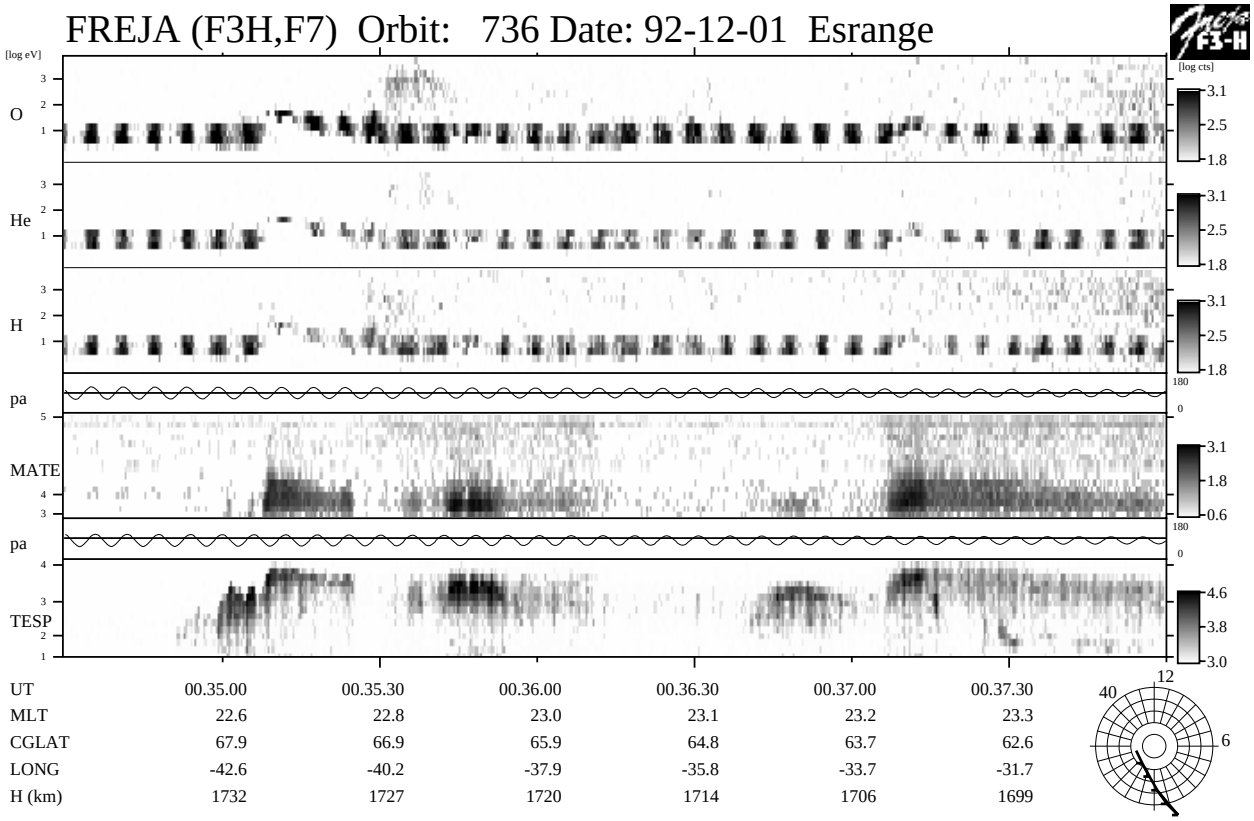

Figure 5.9.2: Three charging events exist around 0035:15 UT, 0035:50 UT, and 0037:15 UT. The electron characteristics appear to be rather similar for these three events (panels 5 and 7).

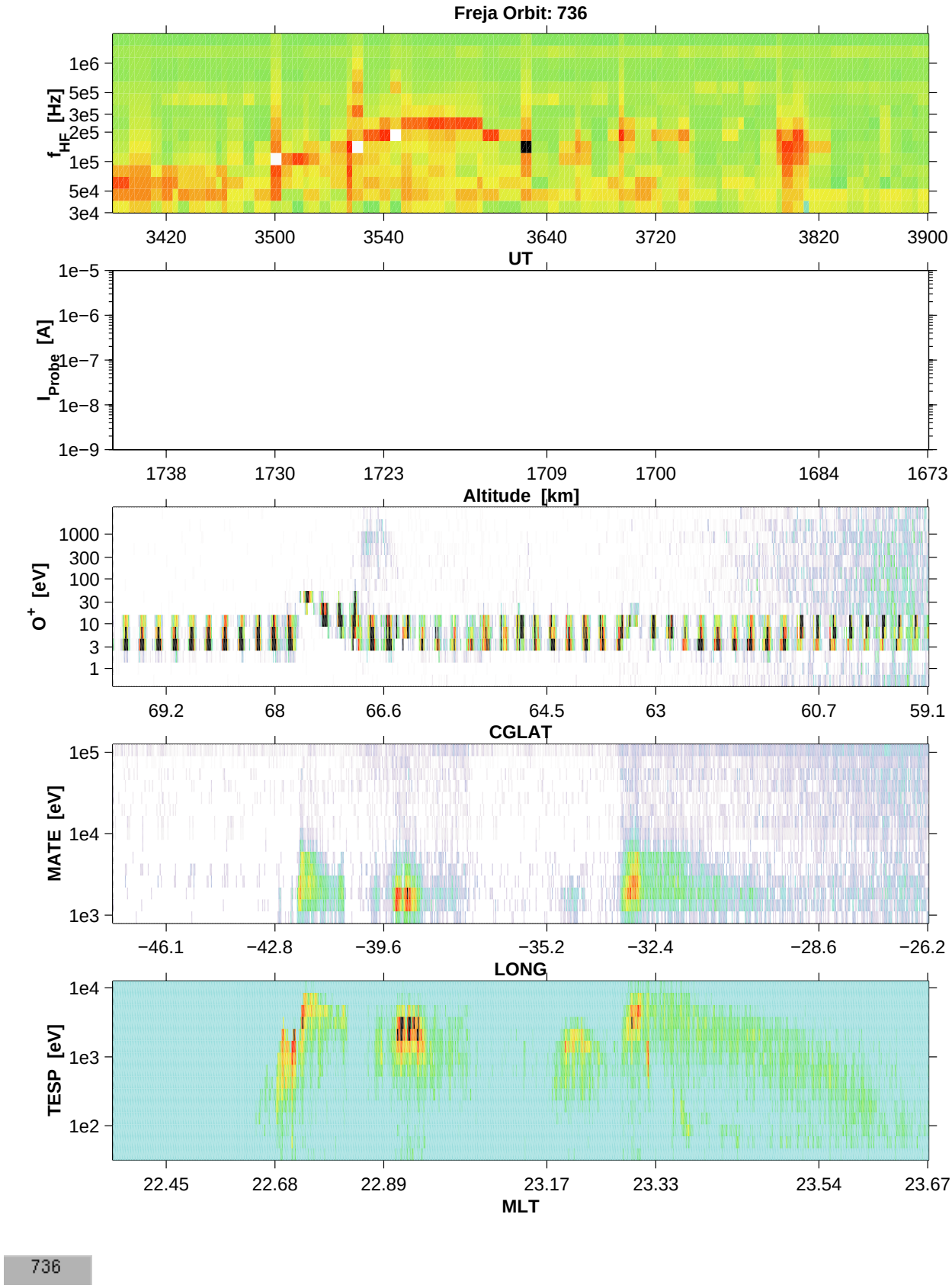

Figure 5.9.3: The electron densities as estimated from the narrow-band HF emissions vary with a factor 5-8, at the same time as the charging level changes by a factor 5-10 (Figure 5.9.2, panels 1-3).

Detailed Particle Distributions

TESP and MATE electron spectra for the charging events are presented in Figures 5.9.4a-d and 5.9.5a-d respectively. Figure 5.9.4a-c shows how the TESP spectra for the first event evolves toward a clear inverted-V type spectra (Figure 5.9.4b, panel 4) with peak energy around 7 - 8 keV for the first event. The electron flux near 1 keV actually decreases at that time. A high energy tail up to about 50 keV is simultaneously developed in the MATE spectra (Figure 5.9.5a, panel 4). The second event (Figure 5.9.4d, panel 2-3) do not reach the same peak energies (more like 3 keV), but has an order of magnitude larger peak flux than the first and the energetic tail is not so developed. It might be so that this larger energetic tail component in the first event is the cause of the charging level difference between the two events. The difference in electron density, i.e. thermal ion return current, might be another reason for the charging level difference. The MATE data from the third event is very similar in its characteristics as the MATE spectra from the first event, and only the difference in plasma density and charging level seems to differ the first and the third events. The TICS data (figure 5.9.1a-c) reveal charging levels of -70 V for the first case and -12 V for the second case.

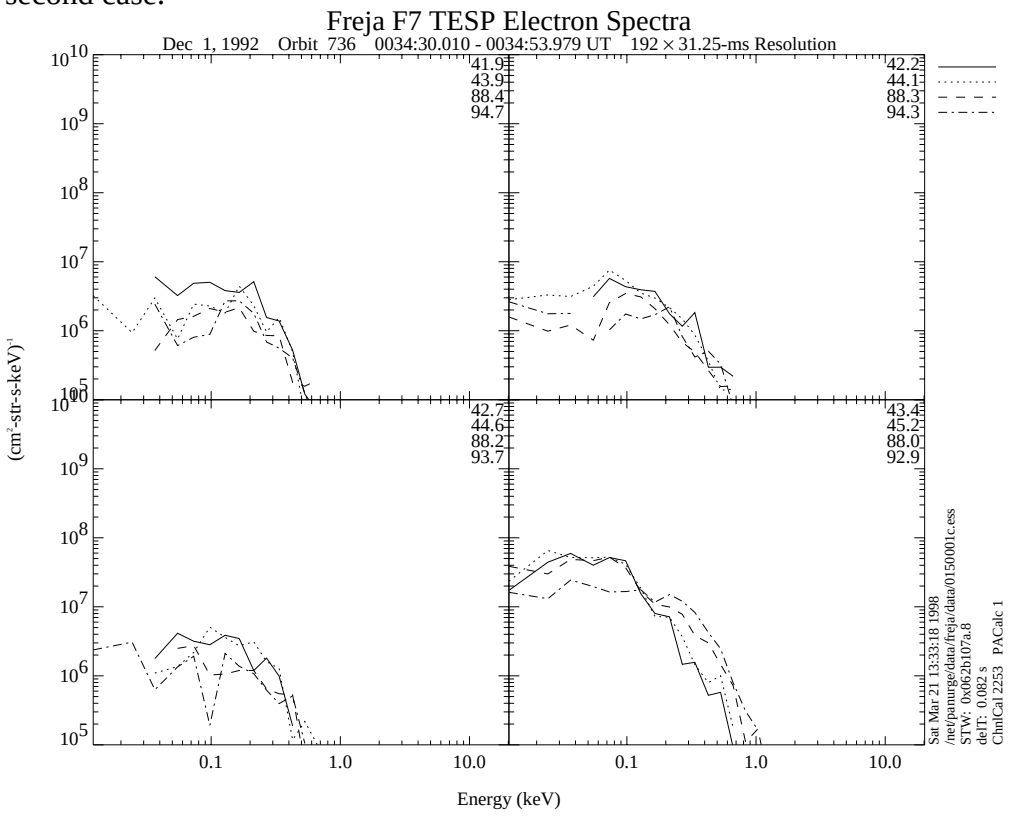

Figure 5.9.4a: TESP and MATE electron spectra for the three charging events are presented in Figures 5.9.4a-d, and Figures 5.9.5a-d. The TESP spectra for the first event evolves toward a clear inverted-V type spectra (panel 4, Figure 5.9.4b) with peak-energy of about 7-8 keV, to be relaxed again in Figure 5.9.4c. The second event is associated with a lower peak energy of about 3-4 keV, but larger flux levels. The MATE spectra of the first event (Figures 5.9.5a-b) show very much the same characteristics as the MATE spectra for the third event (Figures 5.9.5c-d).

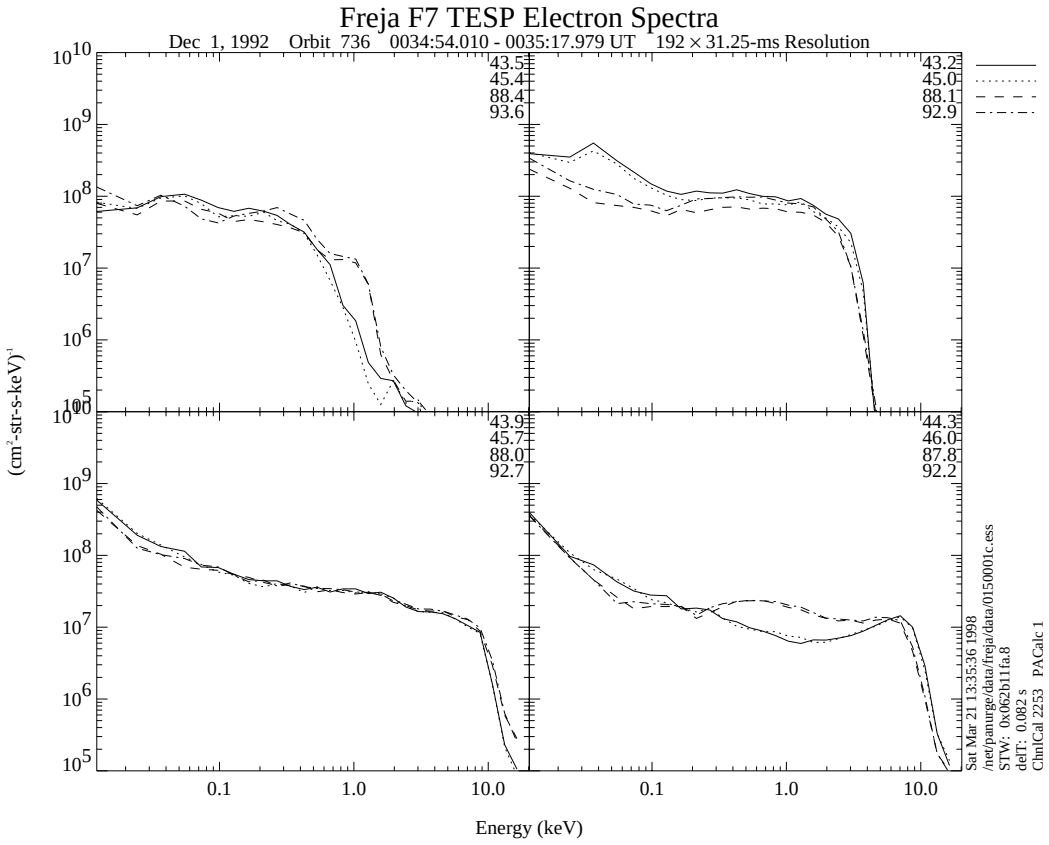

Figure 5.9.4b: TESP spectra from first charging event. See text Figure 5.9.4a.

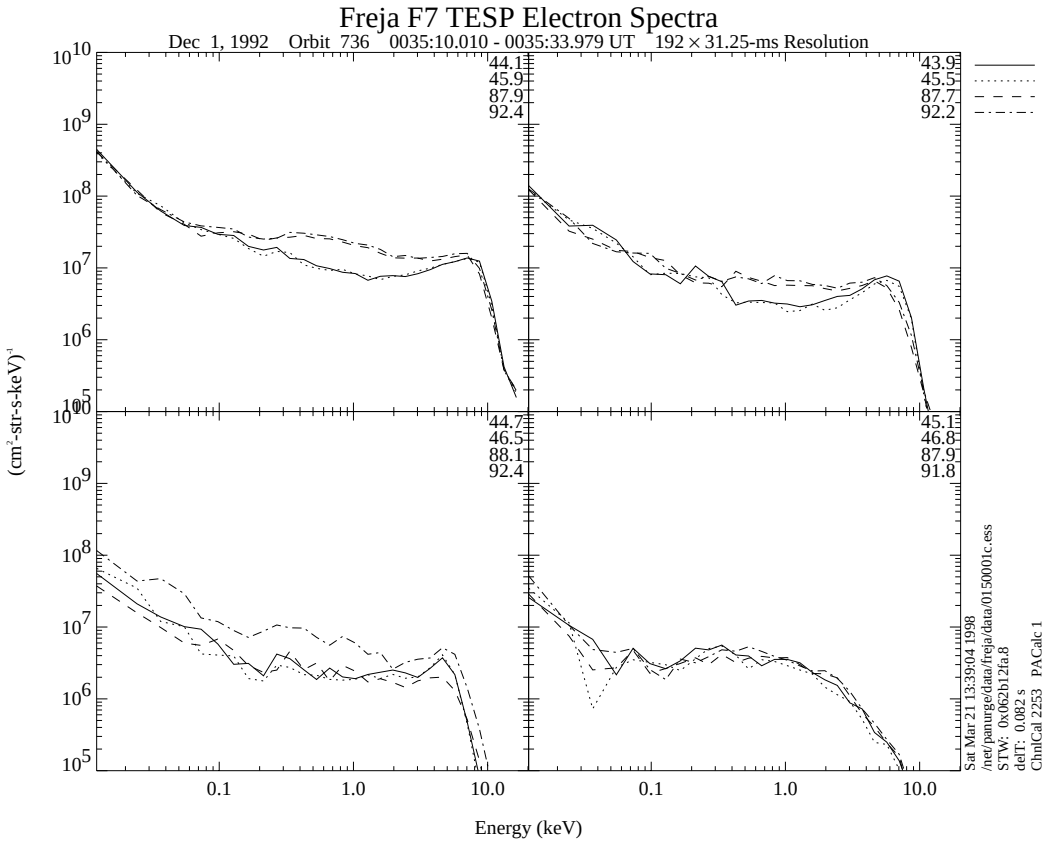

Figure 5.9.4c: TESP spectra from first charging event. See text Figure 5.9.4a.

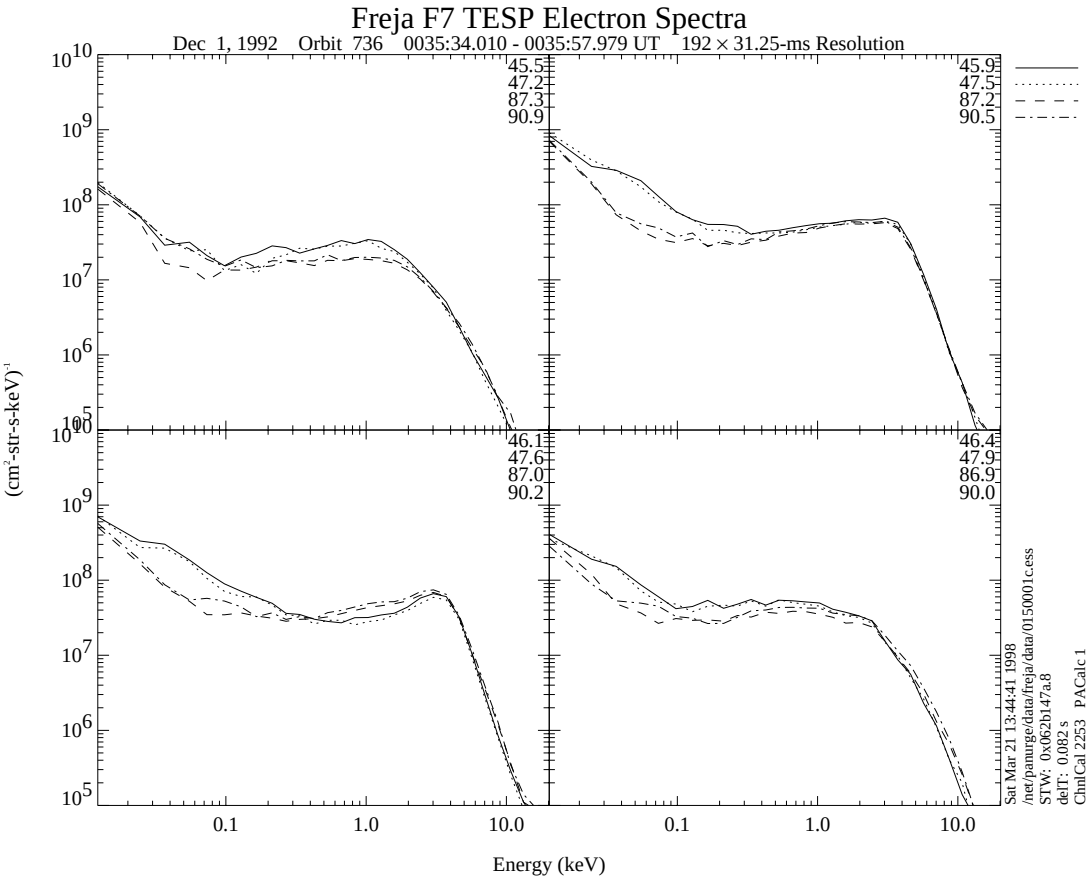

Figure 5.9.4d: TESP spectra from second charging event. See text Figure 5.9.4a.

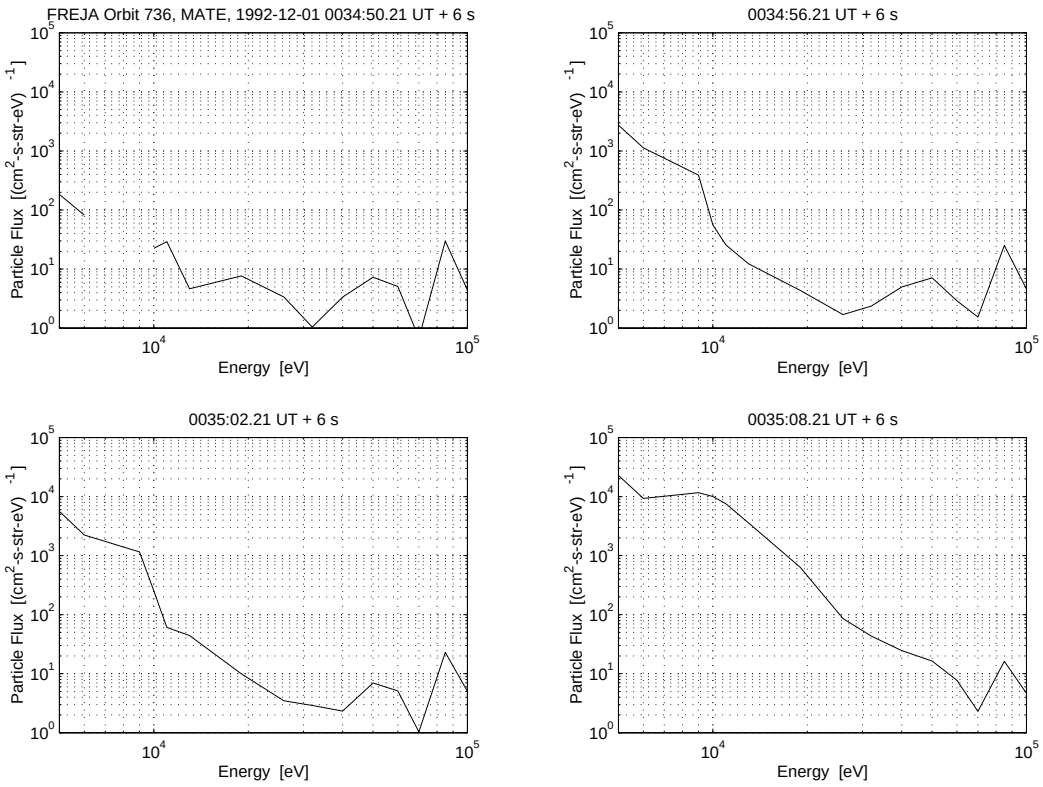

Figure 5.9.5a: MATE spectra from first event. See text Figure 5.9.4a.

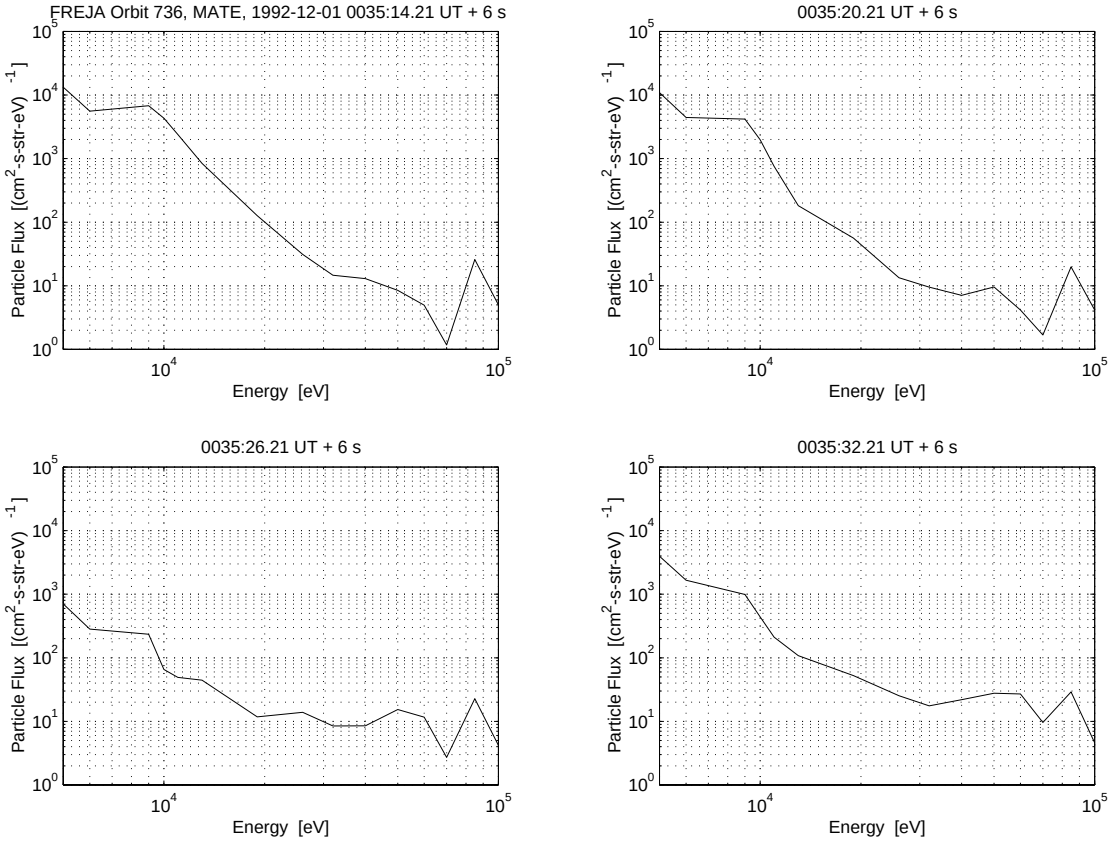

Figure 5.9.5b: MATE spectra from first event. See text Figure 5.9.4a.

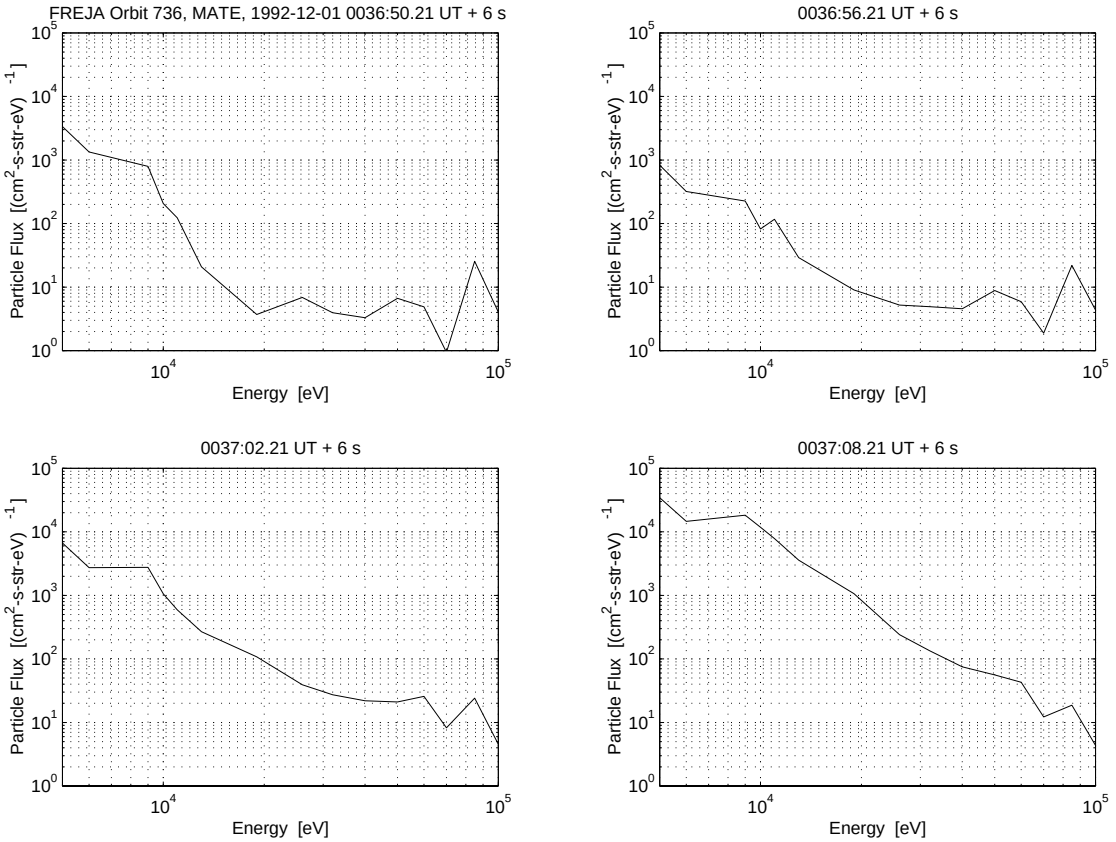

Figure 5.9.5c: MATE spectra from third event. See text Figure 5.9.4a.

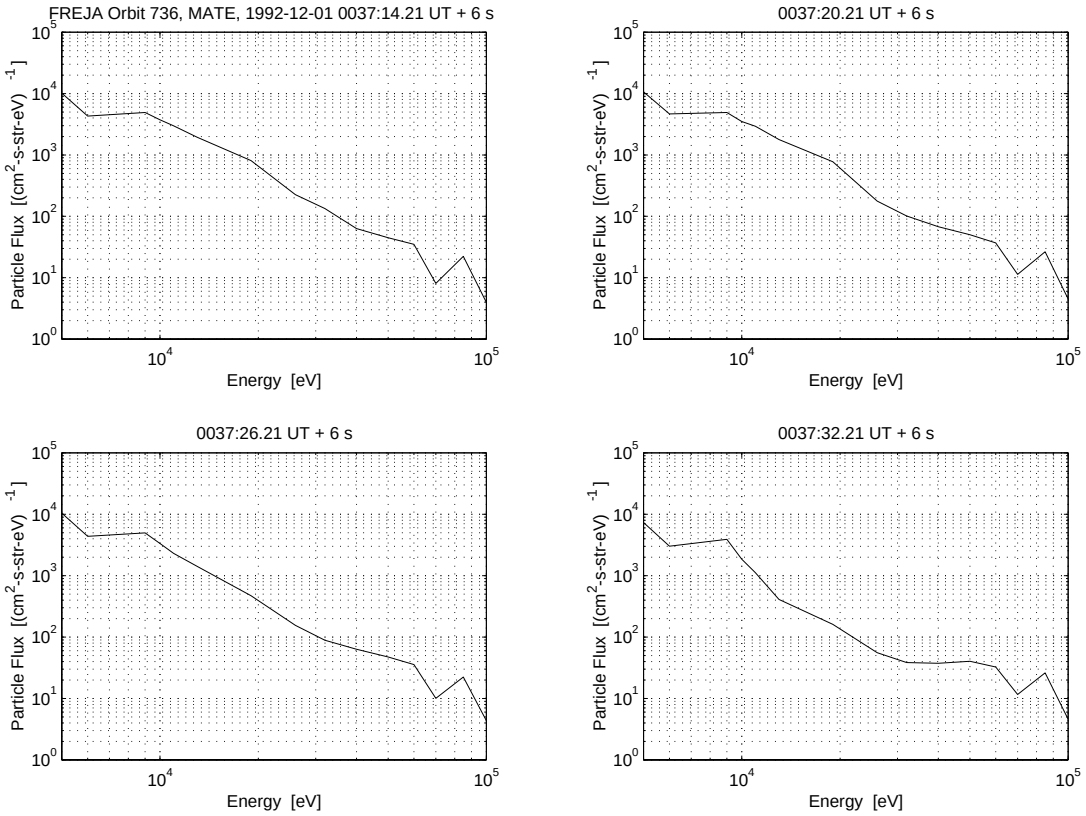

Figure 5.9.5d: MATE spectra from third event. See text Figure 5.9.4a.

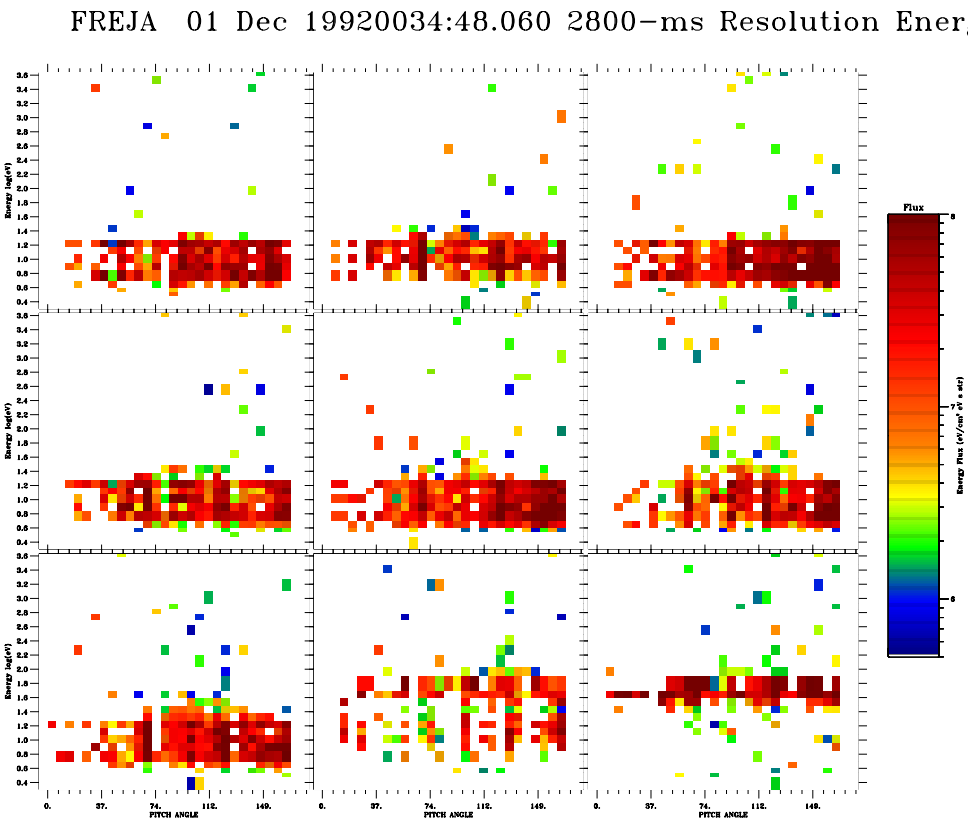

Figure 5.9.6a: Oxygen ion distributions for the first charging event. Negative charging levels of -70 V is inferred.

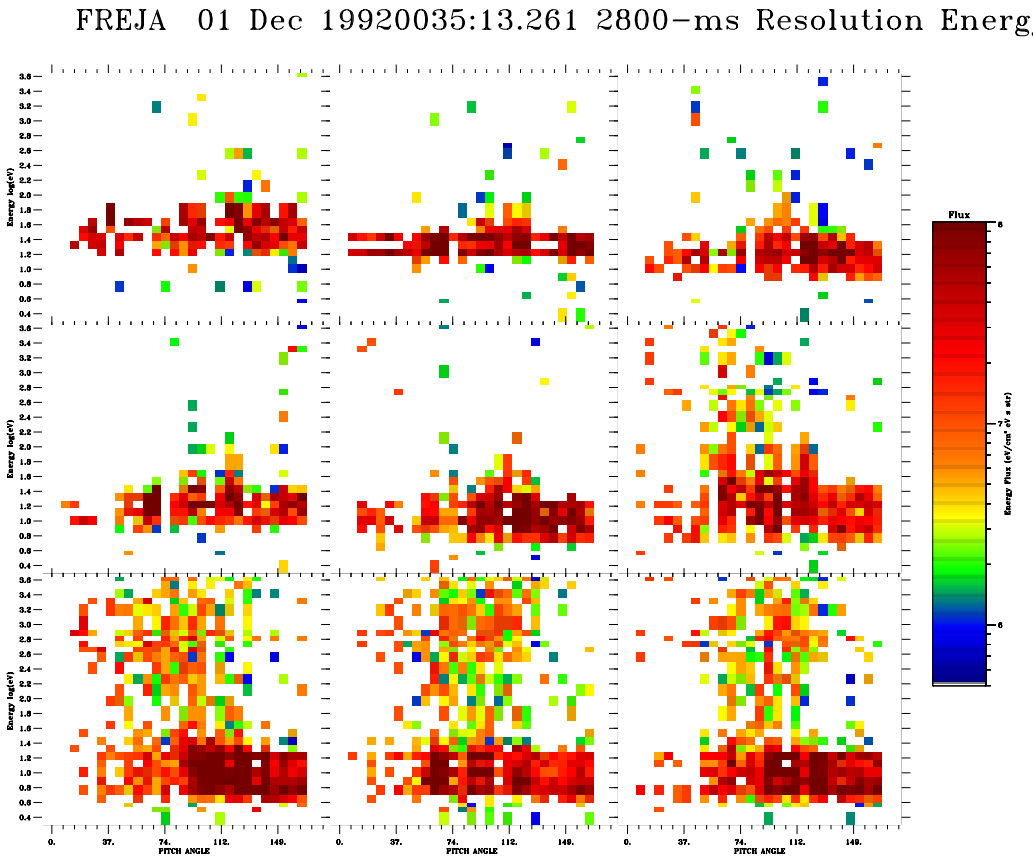

Figure 5.9.6b: Continuation of Figure 5.9.6a.

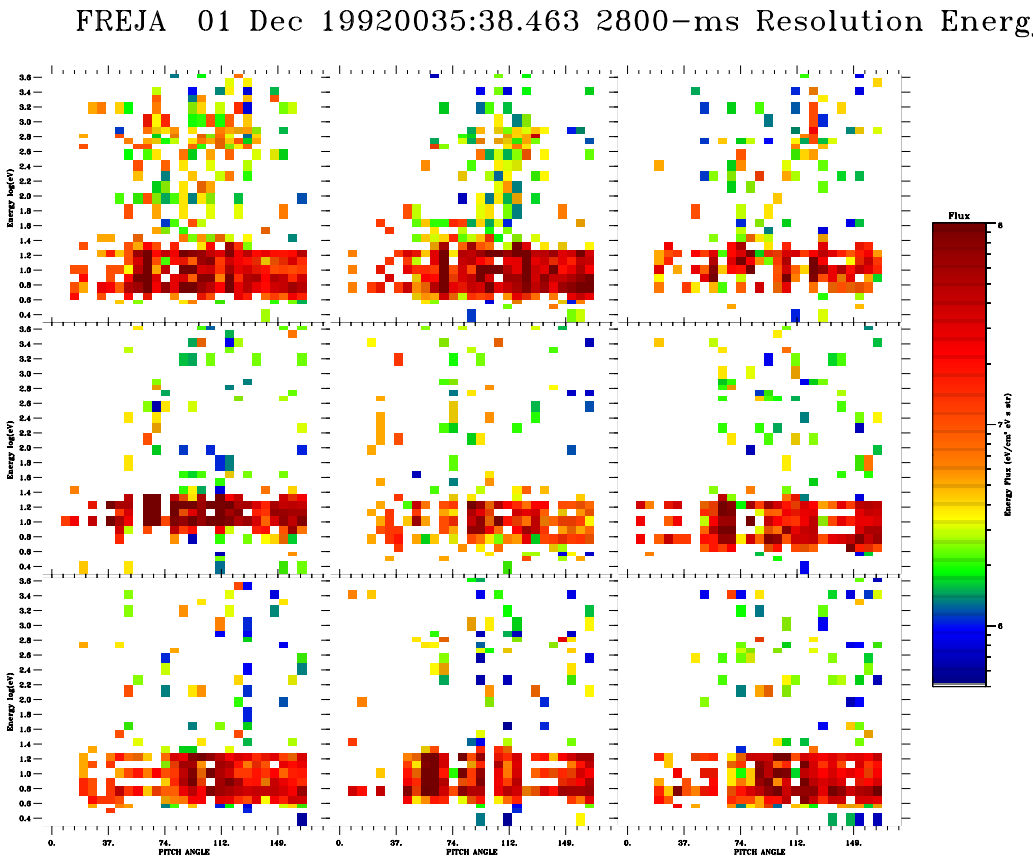

Figure 5.9.6c: Oxygen ion distributions for the second charging event. Negative charging levels of -12 V is inferred.

Conclusions from orbit 736:

- Three cases of Freja charging with rather similar inverted-V electron spectra revealed that the ambient plasma density may affect the charging levels. A change in density by a factor 5-8 seemed to be associated with a change in charging level by a factor 5-10.

5.10 EVENT 10: ORBIT 7279 (LOW ALTITUDE CHARGING)

Overview Data, 94.04.10, Prince Albert

The overview data for the particle measurements from orbit 7279 are presented in Figure 5.10.1, and in somewhat more detail in Figure 5.10.2. The charging event occurs at the rather low altitude of 1395 km during sunlight conditions near 0138:20 UT, which is verified by the UV photometer data (Figure 5.10.3, see also SPEE-WP130-TN). It is the lowest altitude charging event with high resolution Freja data.

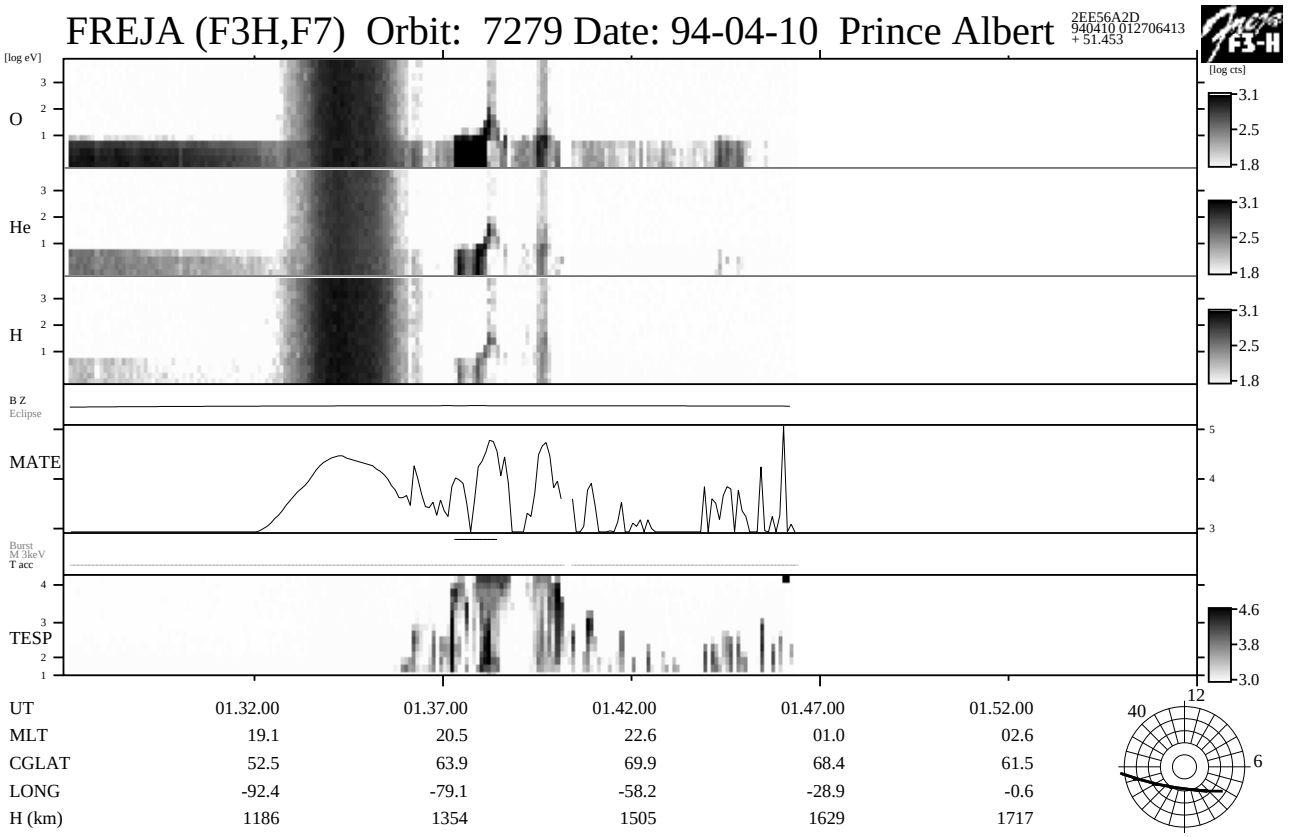

Figure 5.10.1: Overview of the particle data from orbit 7279. The charging event around 0138:20 UT represents the lowest in altitude clearly identified Freja charging event. The event occurs at an altitude of about 1395 km and occurs during sunlight conditions.

The ions (panels 1-3) are lifted to about 20 eV, and a clear inverted-V electron event with superposed low energy suprathermal electron bursts below the inverted-V energies occurs at the same time. The MATE measures only the integrated flux during this orbit. High energy electrons in the MeV range seems to occasionally contaminate the ion data during the charging event. It is interesting to note that the charging increases to its max levels when these supposed MeV electrons exist, while the inverted-V electron spectra just below 25 keV remains constant in its characteristics during the whole charging event. Alternatively, the charging may be inhibited by the lower energy suprathermal electron bursts, by producing secondary electron emission from the Freja surface. The larger charging levels, in fact, occur after these bursts.

An other clear inverted-V event with an even larger peak energy occurs around 0139:40 UT. This later event seems also associated with MeV electrons as indicated from the TICS contamination. Not surprisingly, there is a detectable charging event around this time, even though it is of much lower charging level as compared to the first charging event.

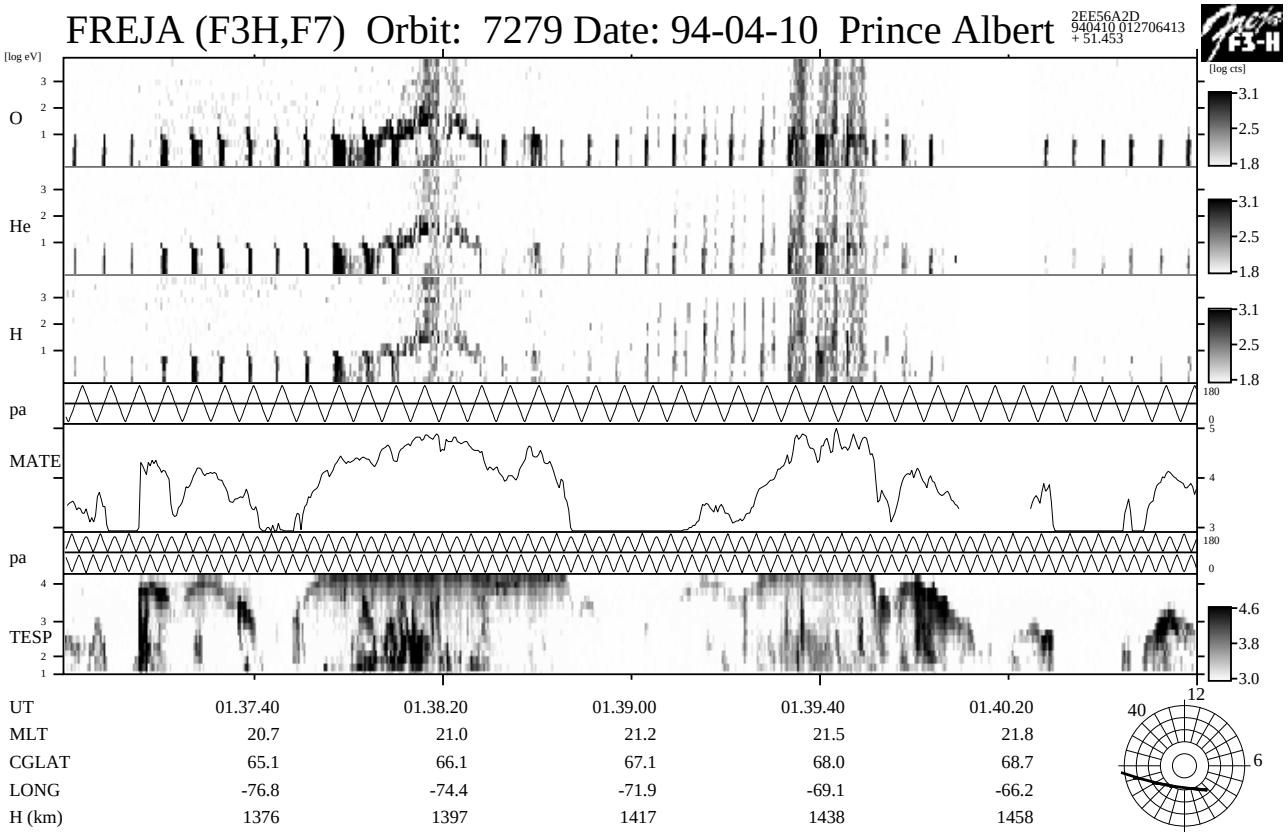

Figure 5.10.2: A blow up of the particle data around the charging event around 0138:20 UT. A clear inverted-V electron event occurs at the same time. The ion channels are contaminated probably by large fluxes of MeV electrons. A similar event which do not seem to be associated with charging occurs around 0139:40 UT.

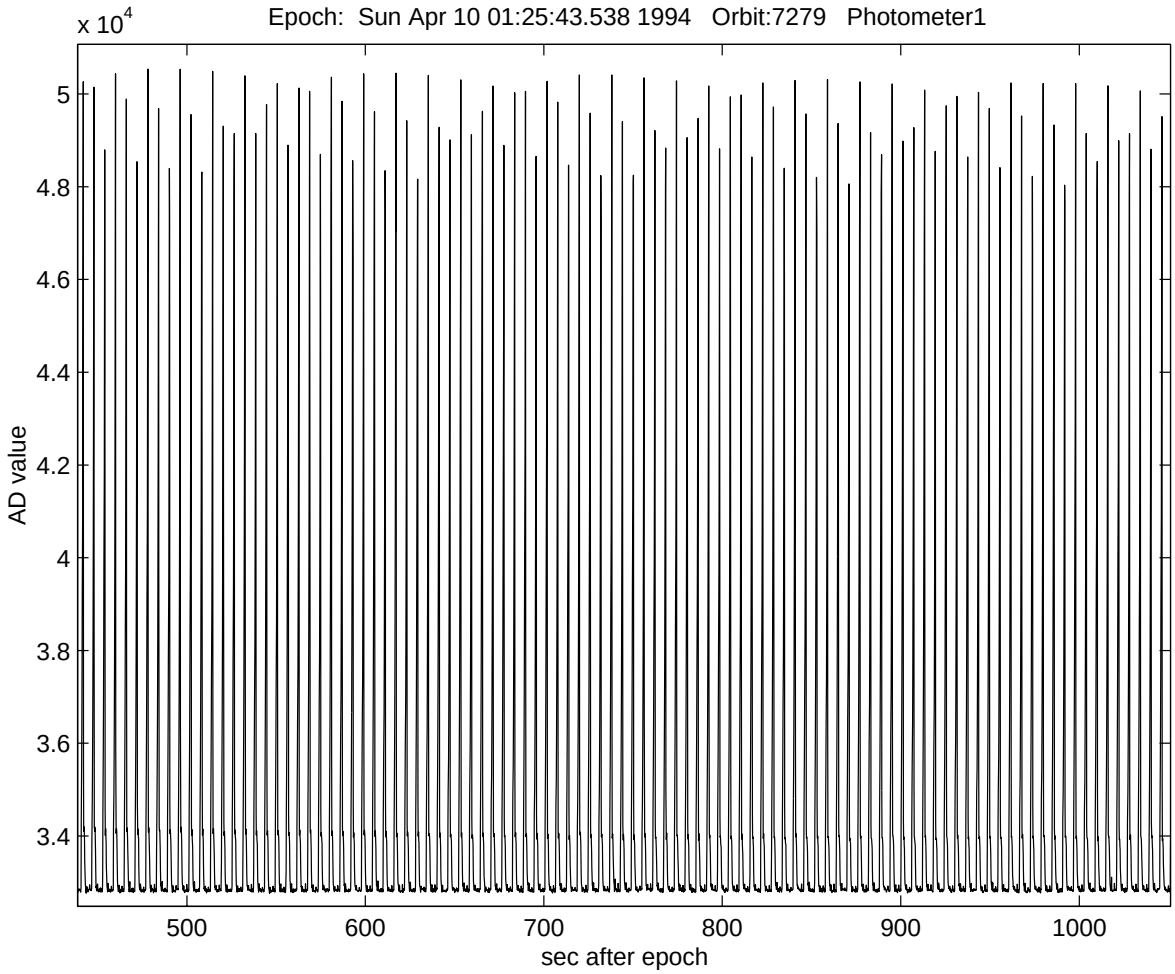

Fig 5.10.3: Photometer data from orbit 7279. Sunlight conditions exist for the whole charging event (750 s to 850 s).

The plasma wave data is displayed in Figure 5.10.4. The inferred density from the narrow-band HF emissions amounts to 7-8·10^8 m^{-3}, which is somewhat lower than the inferred LP density of about 1-2·10^9 m^{-3} outside the charging events.

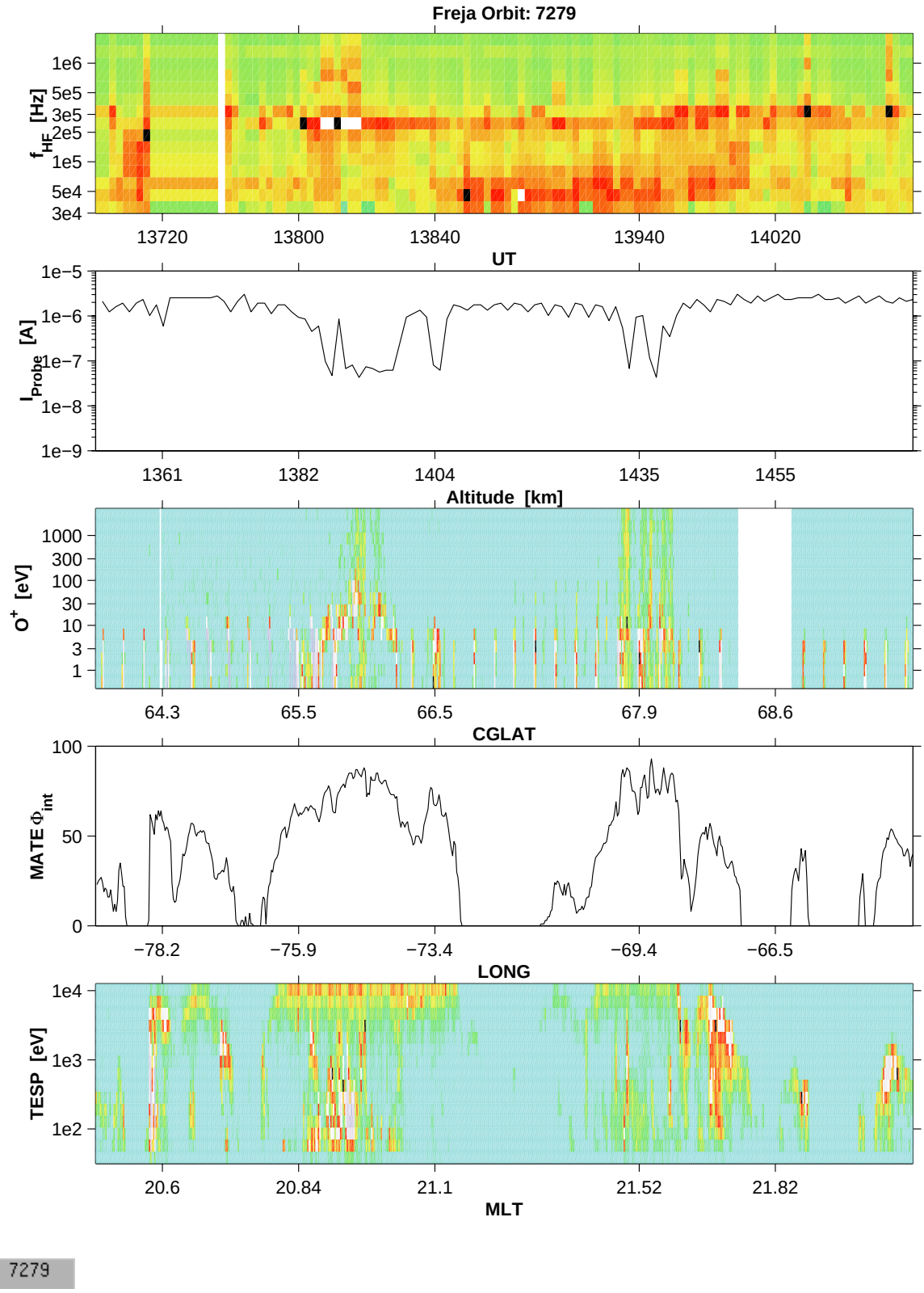

Figure 5.10.4: Plasma wave data corresponding to the particle data in Figure 5.10.2. Rather large plasma densities of close to 10^9 m^{-3} are inferred from the HF narrow-band Langmuir emissions and Langmuir probe current just outside the charging event. Such plasma densities are unusual during charging events, even though densities generally encountered by Freja are a few times this value.

Detailed Particle Distributions

The detailed TESP electron spectra for the time period 0137:48 - 0138:36 UT is displayed in Figures 5.10.4a and 5.10.4b. Unusually many field-aligned suprathermal electron bursts exist below a few keV during this event. Such electron bursts are not common during charging events and are probably unrelated to them since such electrons presumably would rather inhibit the charging process than enhancing it. The inverted-V energy peak is located close to or above the maximum possible measured energy (25 keV). One of the displayed TESP sectors (near 168° pitch-angle) is within the atmospheric loss cone, and therefore shows much lower flux levels above 2 - 3 keV energy.

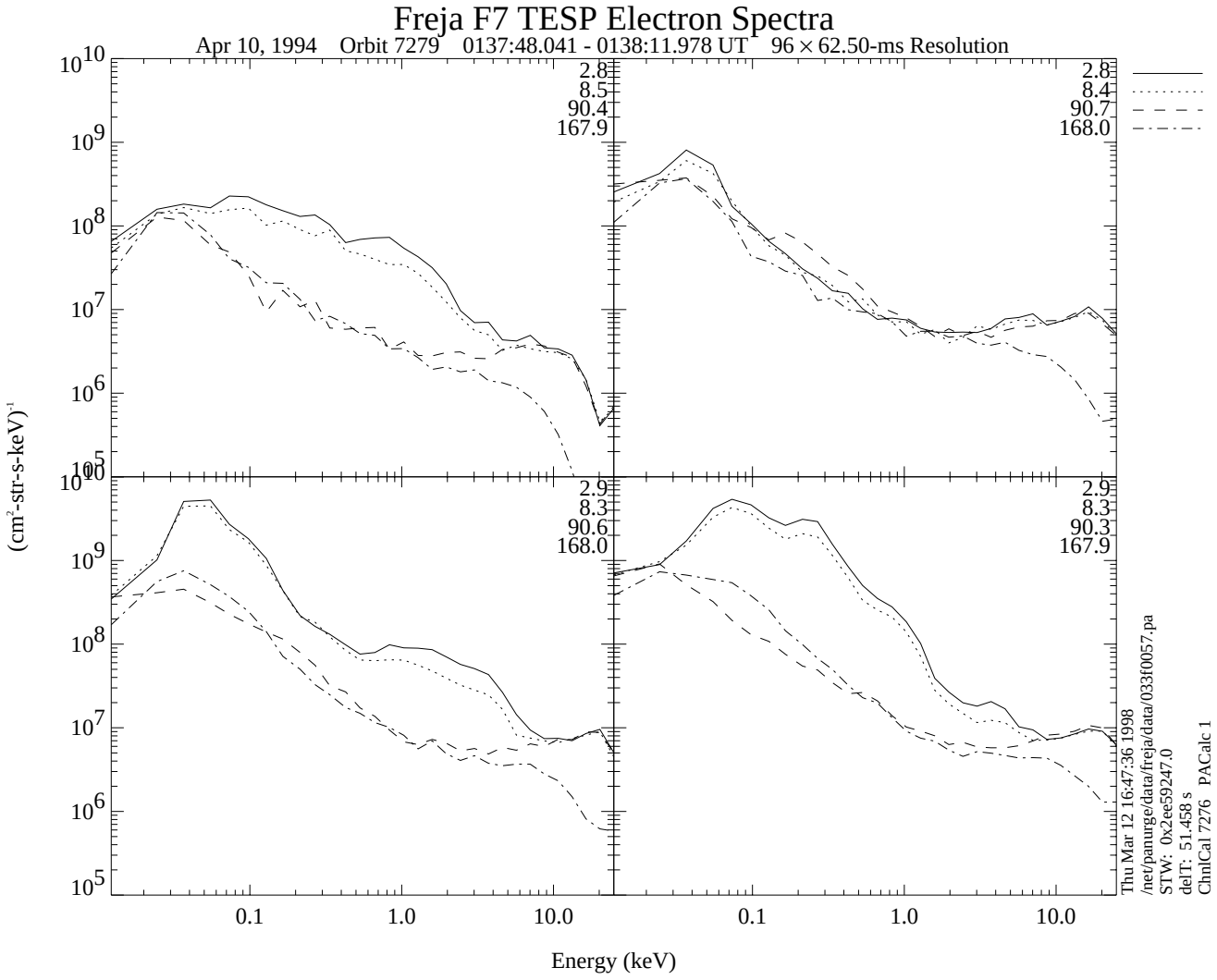

Figure 5.10.4a: TESP electron data from the charging event. Unusually much low energy field-aligned electron bursts appeared during this event. The inverted-V energy peak is close to or possibly above maximum measured energy (25 keV, panels 3-4, this Figure; all panels in next Figure). The 168° channel is measuring within the atmospheric loss cone.

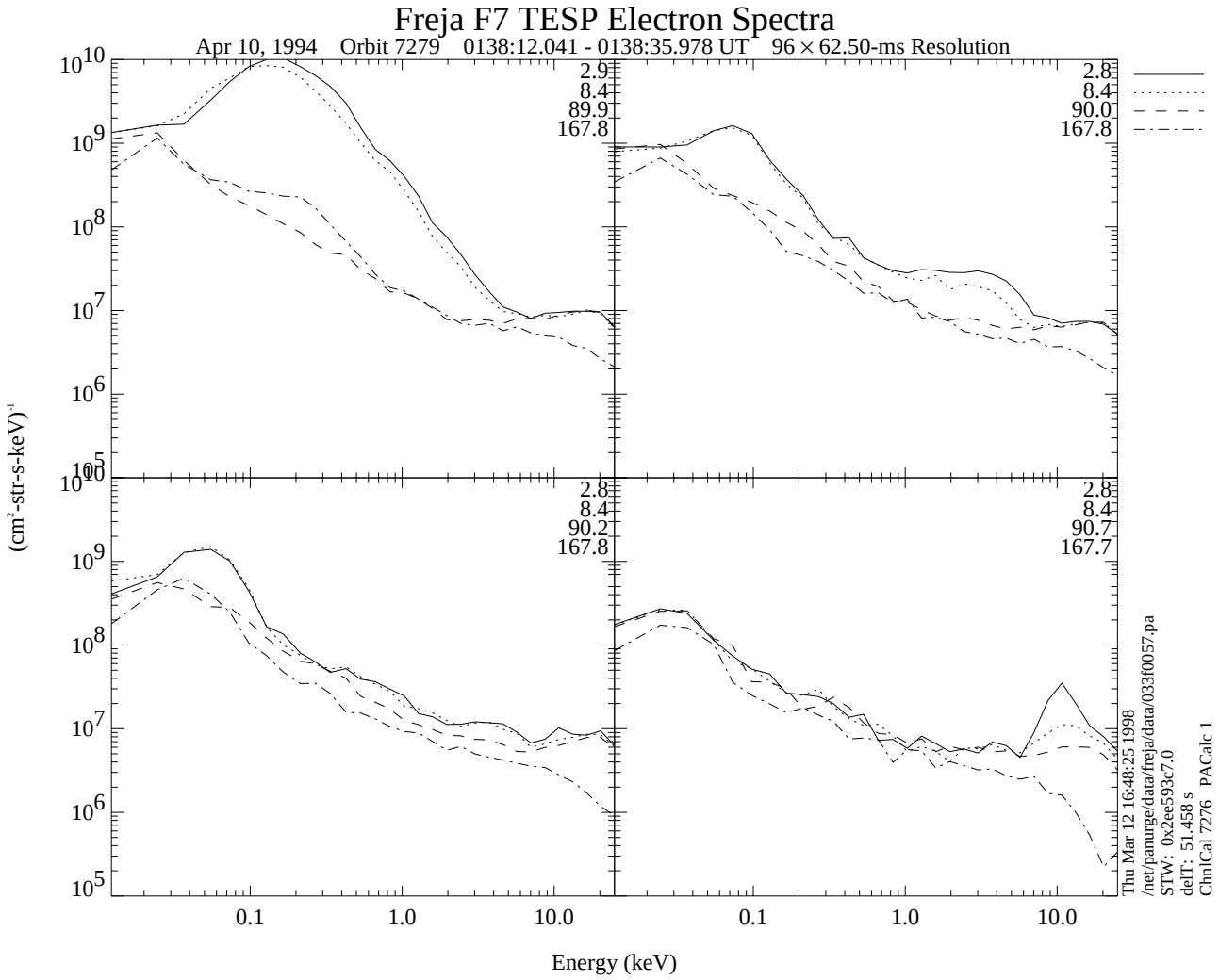

Figure 5.10.4b: See text of previous Figure.

Conclusions from orbit 7279:

- This charging event occurred during sunlight conditions at a low altitude (i.e. somewhat larger magnetic field strength and smaller electron gyro-radii). The gyroradius of emitted photoelectrons (expected to have energies of a few eV) will be 0.1-0.3 m, which is smaller than the size of Freja (about 1.5 m radius). These electrons are therefore expected to return to the spacecraft to a large degree unless large negative potentials accelerate them away from the spacecraft.
- The high energy electron tail seems to enhance the charging levels.
- The influence of low energy suprathermal electron bursts on charging level is not obvious in the data.

6. DISCUSSION OF THE EVENTS

6.1 IDENTIFIED FREJA CHARGING EVENT TYPES

By far the most common type of charging detected on the Freja satellite occurs during high-latitude auroral inverted-V events when extreme fluxes of high energy (5-80 keV or more) electrons hits the spacecraft. Usually the cold ambient plasma density is rather low ($<2 \cdot 10^9$ m^{-3}) during these events, and a majority of these events occured during eclipse. Two other types of charging have been found, but these were associated with very low level charging (< -10 V). One of these just reflects the spacecraft ground potential change when it moves from sunlight to eclipse. An example of such a change in satellite ground potential is shown in Figure 6.1.1 (orbit 709). Almost every sunset/sunrise case have similar charging characteristics; a few Volts negative on the eclipse side and no detectable charging during sunlight conditions. *No charging events of this type has been included in the statistical study [see SPEE-WP130-TN].*

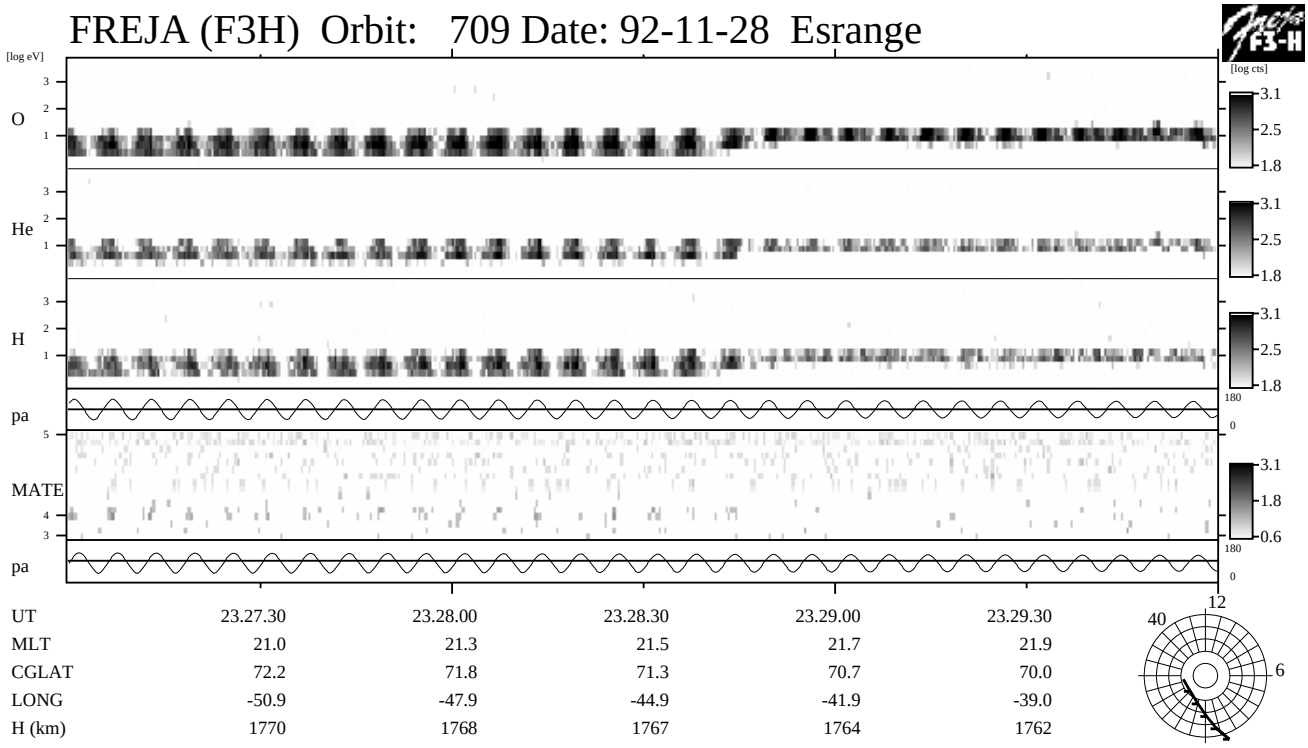

Figure 6.1.1: Overview of the particle data from orbit 709. This event illustrates the normal charging behaviour which occur during every transition from sunlight to eclipse (or vice verse) conditions. A small negative charging of a few Volts appears during eclipse.

The three types of charging detected onboard Freja can therefore be summarised as follows:

- High level charging to about -2000 V associated with energetic electrons in connection with auroral high-latitude inverted-V precipitation events. These can be of two types
    - Eclipse events (most common)
    - Sunlight events (rare, but may still reach high charging levels)
- Low level charging to -10 V due to that the Freja spacecraft enters eclipse conditions during otherwise calm plasma conditions. The photoelectron emission current from the spacecraft disappears when Freja traverses into the darkness, which shift the normal spacecraft potential somewhat to the negative.
- Low level charging to -15 V most probably due to changes in the thermal electron plasma (e.g. electron temperature increase to 2-3 eV perhaps due to heated thermal electrons produced from various plasma instability processes near auroral arcs). There exist unfortunately no data to support this hypothesis for the charging mechanism of these events, and further speculation is therefore meanings-less.

In the continuation all conclusions stated will refer to the first type of auroral (inverted-V) type charging.

6.2 ARCING ?

A majority (if not all) high level charging events detected by the Freja instruments are closely correlated with an increase in the inverted-V peak energy as well as the simultaneous increase in electron flux. This usually occurs over a time span of a few seconds and is therefore not related to sudden discharges (or arcing) in the vicinity of Freja. The charging state of the Freja satellite can therefore be said to have occurred during close to current balance equilibrium conditions, and "violent" discharges have therefore not been confirmed to occur on Freja. This study cannot tell much about so called micro-discharges (micro-arcing) possibly occurring on Freja, because the time resolutions of the Freja detectors are at best 32 ms (TESP), 0.4 s (MATE) and 0.2 s (TICS) respectively.

6.3 COMPARISONS WITH OTHER SPACECRAFT RESULTS

In Chapter 2 the various results from earlier spacecraft studies were addressed, and here we compare them with the results from this study. The Freja satellite was designed to be highly conductive and as electromagnetically clean as possible, and therefore should be better prepared for charging effects compared to the DMSP satellites. The DMSP results suggest that a somewhat lower threshold energy for charging existed and that high level charging could occur at densities an order of magnitude higher than for Freja. Also, the POLAR code simulation results presented in SPEE-WP120-TN indicate that DMSP should be charged to much higher values given the same environment. Yet, the Freja spacecraft achieved somewhat larger max charging levels and did indeed charge during sunlight conditions, which the DMSP satellites never did [*Gussenhoven,* private communication, *Gussenhoven et al.*, 1985]. It should be noted, though, that the Freja mission occurred close to solar minimum, which have been proven to be the most prone period with

regard to charging [*Frooninckx and Sojka*, 1992]. One DMSP result that could not be confirmed by the Freja data was the thermal plasma decrease coincident with most charging events measured by DMSP [e.g. *Yeh and Gussenhoven*, 1987]. We suspect that the plasma density measurements onboard DMSP were jeopardised by the charging events themselves and produced this artefact.

The gyroradius at Freja/DMSP altitudes for around 2 eV secondary electrons are 0.1 - 0.4 m, which is still a significant fraction of the size of Freja. Even so, only a fraction of these electrons will return to Freja through gyromotion, depending on orientation with respect to the Earth's magnetic field direction [*Laframboise*, 1988]. For a larger spacecraft a larger fraction of these secondaries will return to the spacecraft surface, and a larger spacecraft will therefore likely gain somewhat higher charging levels. The same argument is true with regard to sunlight conditions, when large amounts of photoelectrons are emitted from the surface. A smaller spacecraft will not see the photoelectrons return as easily as a larger spacecraft, and the larger spacecraft is therefore more easily charged.

7. CONCLUSIONS FROM THE CHARGING EVENTS CASE STUDY

In this report a detailed description of plasma measurements performed during several Freja electrostatic charging events was given. From this survey, the following observational conclusions can be made:

- All detected charging events were related to the presence of auroral inverted-V energetic electrons, at least down to time scales of the order of 1 second.
- Charging levels up to -2000 kV have been observed in eclipse although the main coating material, Indium Tin Oxide (ITO), is known to have high secondary electron emission properties.
- There exists a clear proportionality between charging level and the rise of the energetic electron peak energy (and the electron flux is most often enhanced an order of magnitude at the peak energy). The highest level charging events have the highest energy peaks and fluxes.
- A high energy tail up to at least 80 keV is observed during the charging events. In some cases large fluxes of MeV electrons occur simultaneously as inferred from the contamination of the ion detector measurements. Such MeV electrons only appears during the most extreme charging events and most probably is the extension of the enhanced high energy tail. MeV electrons could penetrate the upper surface layers and possibly cause internal charging.
- A threshold energy for the inverted-V peak of about 5 keV is inferred, where no charging developed below this value. Even the low level charging events of just a few volts negative were associated with energetic electrons above this threshold.
- Most charging events occurred during eclipse, but a few existed during sunlight conditions. The peak energy threshold were larger (> 10-15 keV) during sunlight conditions.
- Only weak indications exist that low energy suprathermal electron bursts below 1 keV inhibited charging on Freja.
- The thermal plasma density did not usually change significantly when Freja encountered a charging event as compared to the surrounding densities. Also, only weak indications (from orbit 736) exist that the thermal plasma density affected the charging levels significantly.
- The thermal plasma density was rather low ($< 10^9$ m^{-3}) during charging events.
- Several of the plasma instruments showed serious operation disturbances during charging events (above a few tens of volts negative). The Langmuir probe currents dropped to almost zero current due to the fact that few thermal electrons reached the probes. The same effect made the LF and MF plasma wave measurements impossible, and the TICS instrument showed almost ring distributed ions due to the fact that the ions were accelerated toward the spacecraft.
- Transverse ion heating show similar characteristics in the ion spectrometer data (TICS) as those during a charging event. Only careful analysis or the trained eye can easily

differ between the two interpretations.

- No arcing or EMC problems have been identified during the charging events presumably because most of the spacecraft surface was very conductive.

Because Freja was a spacecraft devoted to the scientific investigation of auroral processes, including the measurement of charged particles at low energy, the designers had made special care to provide conductive surfaces of high secondary electron emission material, mainly Indium Tin Oxide (ITO). It has been shown that the charging levels of several thousand volts negative observed occasionally during auroral active conditions may have affected the quality of the data especially for the low energy plasma and the electric field measurements. However, no charging induced problems have been observed on Freja presumably thanks to the careful design regarding conductivity and grounding of the surfaces. However, it should be emphasized that an ordinary spacecraft without strong requirements regarding surface material properties (conductivity, secondary electron emission, …) could have suffered from electrical problems (e.g. arcing) but also an enhanced erosion rate of the surface due to sputtering by the accelerated O^+ ions encountered at low altitude (= 4000 km).

For a high latitude orbiting spacecraft highly conductive surface materials are needed to avoid differential charging and risk of arcing during auroral arcs crossings. To avoid absolute high level charging, surfaces with high secondary electron emission properties are required. The use of ITOC (conductive Indium Tin Oxide Coating) wherever it is possible on the surface appears to be a good regarding electrostatic discharge problems. However, it does not prevent for occasional high level charging. This is because ITOC has a cross over energy of about 2.5 - 3 keV, above which the secondary yield falls below unity, whereas the spectral characteristics of a typical auroral inverted-V events are associated with insignificant low-energy fluxes (< 1 keV) and large fluxes of high energy electrons. These electron events are therefore especially prone to produce high charging levels on *any spacecraft* where the secondary yield crossover-energy for the surface material is a few keV. Search for more appropriate coating materials is a possible line of investigation to mitigate charging. An alternative solution could be provided by active charge control systems, like plasma contactors that are expelling a cold rather dense plasma around the spacecraft. However, such techniques may induce contamination problems and are not recommended onboard spacecrafts used for science.

8. REFERENCES

Anderson, P. C., and H. C. Koons, Spacecraft charging anomaly on a low-altitude satellite in an aurora, J. Spacecraft and Rockets, vol. 33, no. 5, 1996.

André, M., et al., Ion energization mechanisms at 1700 km in the auroral region, J. Geophys. Res., vol. 103, no A3, pp 4199, 1998.

Carlson, M., The Langmuir probes on Freja, IRF Uppsala internal report, 1994.

Carruth, M. R., and M. E. Brady, Measurement of the charge-exchange plasma flow from an ion thruster, J. Spacecraft Rockets, 18(5), 457-461, 1981.

DeForest, S. E., Spacecraft charging at synchronous orbit, J. Geophys. Res., 77, 651, 1972.

Dettleff, G., Plume flow and impingement in space technology, Prog. Aerospace Sci., 77, 3587-3611, 1991.

Eviatar, A., and J. D. Richardson, Corotation of the kronian magnetosphere, J. Geophys. Res., vol. 91, no A3, pp 3299, 1986.

Frooninckx, T. B., and J. J. Sojka, Solar cycle dependence of spacecraft charging in low earth orbit, J. Geophys. Res., vol. 97, no. A3, pp 2985, 1992.

Garrett, H. B., The charging of spacecraft surfaces, Rev. Geophys. Space Phys., vol. 19, no. 4, pp 577, 1981.

Garrett, H. B., and C. P. Pine, Eds., Space systems and their interactions with earth's space environment, vol. 71, Progress in Astronautics and Aeronautics Series, American Institute of Aeronautics and Astronautics, New Nork, 1980.

Gussenhoven, M. S., D. A. Hardy, F. Rich, and W. J. Burke, and H.-C. Yeh, High-level spacecraft charging in the low-altitude polar auroral environment, J. Geophys. Res. vol. 90, no. A11, pp 11009, 1985.

Gussenhoven, M. S., and E. G. Mullen, Geosynchronous environment for severe spacecraft charging, J. Spacecraft Rockets, 20, 26, 1983.

Hall, W. N., P. Leung, I. Katz, G. A. Jongeward, J. R. Lilley, Jr., J. E. Nanevicz, J. S. Tayler, and N. J. Stevens, Polar-auroral charging of the space shuttle and EVA astronaut, in *The aerospace environment at high altitudes and its implications for spacecraft charging and communications*, AGARD-CP-406. p. 34-1, North Atlantic Treaty Organization, France, 1987.

Hastings, D. E., A review of plasma interactions with spacecraft in low Earth orbit, J. Geophys. Res., vol. 100, no. A8, pp 14457, 1995.

Hastings, D., and H. Garret, Eds., Spacecraft environment interactions, Cambridge University Press, Atmospheric and Space Science Series, 1996.

Katz, I., M. Mandell, G. Jongeward, and M. S. Gussenhoven, The importance of accurate secondary electron yields in modelling spacecraft charging, J. Geophys, Res., vol. 91, no A12, pp 13739, 1986.

Katz, I., and D. E. Parks, Space shutle orbiter charging, J. Spacecraft Rockets, 20, 22, 1983.

Koons, H. C., and D. J. Gorney, Relationship between electrostatic discharges on spacecraft P78-2 and the electron environment, J. Spacecraft, vol. 28, no. 6, 1991.

Laframboise, J. G., Calculation of escape currents of electrons emitted from negatively charged spacecraft surfaces in a magnetic field, J. Geophys. Res., vol. 93, no. A3, pp 1933, 1988.

Lazarus, A. J., R. L. McNutt, and Jr., Low-energy plasma ion observations in Saturn's Magnetosphere, J. Geophys., Res., vol. 88, no A11, pp 8831, 1983.

Leach, R. D., and M. B. Alexander, Failures and anomalies attributed to spacecraft charging, NASA Reference Publication 1375, 1995.

Lundin, R., G. Haerendel, and S. Grahn, .Eds., The Freja mission, Space Science Reviews, vol. 70, Nos. 3-4, 1994.

Mullen, E. G., M. S. Gussenhoven, D. A. Hardy, T. A. Aggson, B. G. Ledley, and E. Whipple, SCATHA survey of high-level spacecraft charging in sunlight, J. Geophys. Res., vol. 91, no. A2, pp 1474, 1986.

Newell, P. T., Review of critical ionization velocity effect in space, Rev. Geophys. Res., 23, 93-104, 1985.

Olsen, R. C., A threshold effect for spacecraft charging, J. Geophys. Res., vol. 88, no. A1, pp 493, 1983.

Rosen, A., Spacecraft charging by magnetospheric plasmas, American Institute of Aeronautics and Astronautics, Washington DC, 1976.

Shaw, R. R., J. E. Nanevicz, and R. C. Adamo, Observations of electrical discharges caused by differential satellite charging, in *Spacecraft Charging by Magnetospheric Plasmas*, Prog. Astronaut. Aeronaut., ed. A. Rosen, AIAA Press, New York, 47, 61-76, 1976.

Sittler, E. C., Jr., K. W. Ogilvie, and J. D. Scudder, Survey of low-energy plasma electrons in Saturn's magnetosphere: Voyager 1 and 2, J. Geophys, Res., vol. 88, no A11, pp 8847, 1983.

Stevens, N. J., and M. R. Jones, Comparison of auroral charging predictions to DMSP data, AIAA 95-0370, 33rd Aerospace Sciences Meeting and Exhibit, January 9-12, 1995.

Wahlund, J-E., et al., Broadband ELF plasma emission during auroral energization 1. Slow ion acoustic waves, J. Geophys. Res., vol. 103, A3, pp 4343, 1998.

Yeh, H.-C., and M. S. Gussenhoven, The statistical electron environment for defence meteorological satellite program eclipse charging, J. Geophys. Res., vol. 92, no. A7, pp 7705, 1987.